THE ROLE OF α(1,3)-FUCOSYLATED GLYCANS IN HOMEOSTATIC IMMUNITY, GRANULOPOIESIS AND MUCOSAL INJURY

Lantz C. Mackey

A dissertation submitted to the faculty of The University of North Carolina at Chapel Hill in partial fulfillment of the requirements for the degree of Doctor in Philosophy in the Department of Pathology and Laboratory Medicine.

Chapel Hill
2014

Approved by:

Jonathon W. Homeister

William Funkhouser

Yuri Fedoriw

Yisong Wan

Claire Doerschuk

ABSTRACT

Lantz C. Mackey: The Role of α(1,3)-Fucosylated Glycans in Homeostatic Immunity, Granulopoiesis, and Mucosal Injury.
(Under the direction of Jonathon W. Homeister)

The mechanisms that control granulopoiesis are poorly understood. Mice deficient in α(1,3)-fucosyltransferases (FUT) 4 and 7 ($Fut^{-/-}$) lack selectin ligand activity and selectin-dependent leukocyte trafficking, and have a marked neutrophilia compared to WT mice. These studies utilize mouse models to examine the mechanisms that account for enhanced granulopoiesis in $Fut^{-/-}$ mice and how they alter the pathogenesis of colitis. The results show that $Fut^{-/-}$ mice have elevated circulating IL-17 and G-CSF concentrations, increased prevalence of IL-17-producing cells, and a marked neutrophilia compared to WT mice. Analysis of selectin-deficient mice showed that loss of all three selectins (E-,L-, and P-) induced the neutrophilia and enhanced IL-17 production, similar to $Fut^{-/-}$ mice. These results suggest that loss of Fut-dependent selectin-mediated leukocyte trafficking alters granulopoiesis by modulating a previously proposed IL-17-dependnent granulopoietic regulatory loop.

Experiments using bone marrow transplants, adoptive neutrophil transfer, and myeloid-specific alteration of FUT7 expression revealed that

BM-derived myeloid cell trafficking is primarily responsible for regulating granulopoiesis. In vitro analysis of BM-derived and tissue resident phagocyte populations reveal no defect in phagocytosis or IL-23 production in $Fut^{-/-}$ mice. Together these results suggest Fut-dependent selectin-mediated myeloid cell trafficking, not tissue phagocyte function, regulates granulopoiesis.

DSS-induced murine colitis is largely dependent on the innate immune system and is exacerbated by elevated IL-17. Compared to WT, colitis in $Fut^{-/-}$ mice was more severe, determined by weight loss, occult bleeding, and histology. The role of Tcell-derived IL-17 in the development of colitis was examined using $Rag1^{-/-}/Fut^{-/-}$ deficient mice. Absence of Tcells and Bcells did not alter disease severity in $Fut^{-/-}$ mice.

The results from these studies highlight the importance of Fut-dependent leukocyte trafficking of BM derived myeloid cells in regulating IL-17-dependent granulopoiesis and modulating disease severity in DSS-colitis. Taken together these studies demonstrate that leukocyte trafficking is required to maintain homeostatic immunity, and that disruption can lead to significant alterations in the inflammatory state.

DEDICATION

I would never have been able to finish this project without the love and support of my family and friends, especially my wife Laura, and my children Lantz and Ashleigh.

TABLE OF CONTENTS

List of Tables

List of Figures

List of Abbreviations

BM: Bone Marrow

BM-MC: Bone Marrow Derived Macrophage

BM-DC: Bone Marrow Derived Dendritic Cell

pKC: Primary Kupffer Cell

ILC: Innate Lymphoid Cell

NKT: Natural Killer Tcell

IL-: Interleukin-

Fut: Fucosyltransferase

EG: Emergency Granulopoiesis

RPM: rotations per minute

PBS: Phosphate Buffered Saline

HBSS: Hanks Balanced Salt Solution

qPCR: Quantitative Polymerase Chain Reaction

mRNA: messenger RNA

cDNA:

n: Number

$Fut^{-/-}$: Fut4 and Fut7 Deficient Mice

DSS: Dextran Sulphate Sodium

Chapter 1 – Background and Introduction

1.1 Fucosyltransferases

The Fucosyltransferases (FUTs) are a family of glycosylating enzymes found in the Golgi that are responsible for catalyzing the addition of a fucose moiety to a protein or glycan[1]. To date there have been 12 distinct fucosyltransferases identified in humans with various substrate specificities and tissue expression patterns[2-4]. Of the 12 FUTs identified in humans, nine murine homologs have been identified with similar sequence, structure and function to human FUTs[4].

FUTs are classified by the manner in which they link the fucose moiety to the developing glycan. FUTs 1 and 2 catalyze the addition of a fucose in α(1,2) linkage to a glycan chain and are responsible for synthesis of the blood group antigens in both humans and mice (Figure 1.1)[2, 4]. FUTs 3, 4, 5, 6, 7, 9, and 11 catalyze the addition of a fucose using an α(1,3) linkage. In mice FUT 3 is a pseudogene with no known function, and FUTs 5 and 6 have not been identified[2]. FUTs 4 and 7 are expressed in myeloid cells and are responsible for the formation of sialyl Lewis x, which is a component of all selectin ligands and is required for high affinity selectin binding[1, 7-9]. FUT 9 has been shown to be

expressed predominately in the brain, skin and at low levels in peripheral blood leukocytes and is involved in the production of the Lewis x and Lewis y antigens[2, 3]. FUTs 10 and 11 have been identified but to date their functions and specificity remain unclear[2]. FUT 8 utilizes an $\alpha(1,6)$ linkage to fucosylate the μ heavy chain of the B-cell receptor and is required for proper B-cell development[2, 3]. PoFUT 1 is unique, in that it catalyzes the addition of an O-linked fucose directly to a peptide chain. PoFUT 1 has been shown to be involved in fucosylation of Notch ligands, which are integral to controlling thymocyte development[2, 4, 10].

Fut4 and Fut7 are of particular importance in regards to leukocyte trafficking. As stated above, these enzymes are widely expressed in leukocytes and are responsible for the formation of sialyl Lewis x on the selectin ligand that is required in part for recognition by the carbohydrate binding domain on the selectin. Mice deficient in FUT4 and FUT7 ($Fut^{-/-}$) have been shown to have a severe selectin-dependent leukocyte trafficking deficiency[1, 8, 9].

1.2 Selectins

The selectins are a family of adhesion molecules that mediate leukocyte rolling. Selectin recognition of, and binding to, their ligands is a crucial initial step in leukocyte trafficking to sites of infection and inflammation, and lymphocyte homing to secondary lymphoid organs. P-

and E- selectins are expressed on the activated endothelium and interact with their ligands (i.e. P-Selectin Glycoprotein Ligand -1, PSGL-1) expressed on the cell surface of circulating leukocytes, and are responsible for the initial stages of leukocyte extravasation[1, 7-9]. L-selectin is expressed on leukocytes and is required for lymphocyte homing to peripheral lymph nodes via the high endothelial venules[7]. Studies have shown that selectins and their ligands are post-translationally glycosylated. During glycosylation of selectin ligands, FUT4 and FUT7 catalyze the addition of a fucose moiety to the glycan chain completing the formation of sialyl Lewis x (sLex), which is essential for the high affinity interactions between selectins and their ligands[1, 2, 9]. Mice doubly deficient in FUT4 and FUT7 are unable to produce functional E-, P-, or L-selectin ligands. Studies using these mice have demonstrated that the loss of selectin ligand activity leads to reduced leukocyte migration, altered inflammatory responses, a pro-thrombotic state, and a pronounced leukocytosis with neutrophilia[1, 2, 4, 7-9].

1.3 Granulopoiesis

Neutrophils are a phagocytic cell of the innate immune system. These cells are found in large numbers in peripheral blood and tissues[11-13]. It is believed that neutrophils have a short half-life ranging from 12 - 36 hours in circulation, after which they traffic into

peripheral tissues where they are phagocytosed and degraded[14-17]. Under inflammatory conditions neutrophils are rapidly recruited to sites of infection and injury where they phagocytose bacteria and cellular debris, release various proinflammatory mediators and antibacterial peptides (perforin & granzyme), and secrete matrix-modifying enzymes (MMP8)[12, 13]. These cells are considered the 'front line' in the immune system, and patients with reduced neutrophil counts are at serious risk for infection[12, 18, 19]. Due to the neutrophil's short lifespan yet vital function, they must be constantly produced to ensure an adequate supply in the blood stream. Granulopoiesis, or the process of neutrophil differentiation and maturation, occurs in the bone marrow as hematopoietic stem cells undergo several differentiation steps until terminal differentiation into mature neutrophils[14, 20].

Despite the importance of granulopoiesis, the detailed regulatory network modulating this process has not been fully described. However, recent studies have demonstrated that impaired leukocyte trafficking can drastically alter granulopoiesis[11, 12, 14, 15, 17, 20]. An elegant series of experiments led to the proposal of a feedback loop that regulates granulopoiesis (Figure 1.2)[20]. This model suggests that the extra-vascular neutrophils in peripheral tissues undergo apoptosis and are taken up by macrophages and dendritic cells. This efferocytosis (phagocytosis of an apoptotic neutrophil) reduces IL-23 production by

resident macrophages and dendritic cells. IL-23 stimulates IL-17 production by various leukocyte populations, which in turn increases Granulocyte-Colony Stimulating Factor (G-CSF) production[20]. Changes in G-CSF production control the rate at which neutrophils differentiate, mature, and are released from the bone marrow. Alteration of IL-23, IL-17, or G-CSF production or signaling can severely alter granulopoiesis and thereby the ability of the innate immune system to respond to infection or tissue damage[19-24].

1.4 Modulation of Granulopoiesis by Leukocyte Trafficking

The ability of leukocytes to traffic out of the vasculature and into the periphery to patrol for tissue damage or infection is a key component of the innate immune system[1, 9, 20]. Blocking proper trafficking of neutrophils, macrophages, and/or dendritic cells leaves animals with an elevated risk for infection[11, 13, 18, 19, 25]. Impairment of neutrophil trafficking reduces the number of neutrophils that enter the tissue, phagocytose cell debris or bacteria, and undergo apoptosis[26]. Efferocytosis has been shown to result in potent anti-inflammatory effects[27-34]. For example, efferocytosis induces IL-10 and TGF-β production, reduces IL-23 and TNF-α production, and increases alpha defensin levels[27, 28, 35, 36]. However, the underlying mechanisms leading to these responses remain unclear.

During efferocytosis, the key response that modulates granulopoiesis is the reduction or cessation of IL-23 production by macrophages and dendritic cells[11, 17, 20, 27, 36-39]. In the case of a neutrophil trafficking deficiency (as seen in mice lacking FUT4 and FUT7) efferocytosis in the periphery should be reduced, resulting in enhanced IL-23 production, leading to elevated rates of granulopoiesis.

1.5 IL-23 Production and Effector Function

IL-23 is a member of the IL-12 family of cytokines[36]. It is a heterodimeric cytokine made up of a conserved p40 subunit (shared with IL-12) and a unique p19 subunit[36]. Production of IL-23 can be induced following Toll-Like Receptor (TLR) recognition of bacterial products (i.e. LPS or peptidoglycan), Dectin-1 receptor recognition of fungal β-glucans, or via CD40/CD40L interaction[36, 38]. Secreted IL-23 will bind to the IL-23 receptor that is made up of an IL-12Rβ1 subunit (which recognizes the p40 domain) and the IL-23 subunit (which recognizes the p19 domain)[36, 40, 41]. IL-23R expression is controlled by the transcription factors RORα and RORγt which are only expressed in specific lymphoid cells: Th17 Tcells, $\gamma\delta$ Tcells, some Natural Killer Tcells (NKT cells), and Innate Lymphoid cells (ILCs)[39, 41, 42]. Binding of IL-23 to IL-23R causes the activation of an intracellular signaling cascade through Janus associated kinase (Jak)/ signal transducer activator of

transcription (STAT) signaling. Jak2 and tyrosine kinase 2 (Tyk2) will phosphorylate the IL-23R complex, creating binding sites for STATs 1, 3, 4, and 5 which become phosphorylated, dimerize and translocate to the nucleus to drive the transcription of STAT-responsive genes[39, 42, 43]. In general, IL-23 signaling induces a proinflammatory response, however the precise nature of the response depends on the specific cell type that has been activated[41, 44, 45]. In lymphocytes, STAT3 is preferentially phosphorylated while STAT4 and STAT5 are weakly phosphorylated[42, 46]. This results in activation of an IL-17-producing phenotype in subsets of lymphocytes.

1.6 IL-17 Production and Effector Function

IL-17 is a recently identified cytokine that has been implicated in inflammatory and autoimmune diseases ranging from asthma and multiple sclerosis, to defense against fungal infections[10, 47]. IL-17 production by Th17 Tcells, γδ Tcells, NKT cells, and ILCs is induced by IL-23 stimulation of the IL-23R, or by the combined stimulation of IL-6 and TGF-β[20, 41, 43, 48, 49]. Stimulation of these receptors results in the activation of Jak2, which phosphorylates STAT3. After activation by phosphorylation, STAT3 forms a heterodimer and translocates to the nucleus to drive the transcription of the orphan nuclear receptor RORγt, which is responsible for initiating the transcription of IL-17a, IL-17f, IL-

22, and IL-23R[10, 22, 47, 50, 51]. While RORγt has been shown to be the key transcription factor responsible for controlling IL-17 production, it does interact with several enhancer proteins (NFAT, Batf, c-Maf, AhR, and RUNX1) that amplify IL-17 production[10, 42]. The ability of IL-17-producing cells to upregulate IL-23R allows these cells to perpetuate an IL-17 response, in an autocrine and paracrine manner.

After secretion, IL-17 binds to the IL-17RA/IL-17RC complex, causing the phosphorylation of Act1[10, 42]. The kinases down stream of Act1 that are involved in transducing the IL-17 signal have yet to be fully elucidated, however it is clear that IL-17 can activate the NF-κB, MapK, and C/EBPα/β signaling pathways[50-53]. While IL-17R signaling can stimulate the expression of many target genes, the most relevant for granulopoiesis is C/EBP-dependent expression of G-CSF[22, 37, 39, 51].

1.7 G-CSF Production and Effector Function

G-CSF is a key growth factor that controls the survival, proliferation, and maturation of neutrophils[6, 14]. G-CSF production can be induced in stromal cells following stimulation with IL-17, LPS, TNFα, or IL-1β [25]. Activated C/EBPβ and NF-κB p65 binds to the G-CSF promoter to drive its transcription[25, 54, 55]. After secretion, G-CSF binds to the G-CSFR, which is expressed on myeloid progenitors, endothelial cells, cardiomyocytes, granulocytes, and some monocytes.

The G-CSFR signals by activating Jak1 and Jak2, creating binding sites for STAT1, STAT3, and ERK1/2[25, 54, 55]. While STAT3 is thought to be responsible for stimulating granulocyte maturation and release under normal conditions, experiments revealed a pronounced neutrophilia in STAT3-deficient mice instead of a neutrophil deficiency[25, 55]. The investigators hypothesized that in the absence of STAT3, suppressor of cytokine signaling (SOCS) 3, which inhibits STAT signaling, remains inactive allowing STAT1 and ERK1/2 to continuously stimulate neutrophil release from the bone marrow [55]. G-CSFR signaling activates a diverse set of target genes responsible for accelerating cell cycle progression and proliferation (Cyclin D3), enhancing neutrophil maturation (c-fos, IRF-1, PU.1), enhancing neutrophil effector function (FcγII/III , Mac1), and promoting neutrophil survival[11, 14-16, 25, 54-56].

1.8 Emergency Granulopoiesis

In addition to steady-state regulated homeostatic granulopoiesis, the body must be able to rapidly respond to infectious stimuli by greatly expanding production and release of neutrophils. This process of rapid *de novo* production of neutrophils is called emergency granulopoiesis (EG)[6, 25]. While the result of EG is similar to normal granulopoiesis, it is thought to have distinct separate signaling mechanisms that override

bone marrow production of other cell types, and focus on the production of neutrophils[57, 58].

Activation of EG can occur directly or indirectly. Direct activation occurs when bacterial components (LPS, PAMPS) are recognized directly by the hematopoietic stem cells (HSCs)[59]. In the case of LPS activation of TLR4, myd88 is phosphorylated and activates NF-κB and AP-1 signaling, promoting proliferation of HSCs and IL-6 production[60, 61]. These factors promote granulopoiesis and suppress lymphopoiesis[6]. Indirect activation of EG occurs when bacterial products are recognized by pattern recognition receptors (PRRs) on peripheral leukocytes or certain non-hematopoietic cells (endothelial cells)[62, 63]. Activation of these cells causes the production of various cytokines, including IL-6 and G-CSF. Under infectious conditions levels of G-CSF are significantly elevated resulting in increased G-CSFR signaling (Figure 1.3.) [6, 25, 58, 64-66].

Regardless of which method stimulates EG, they both result in the activation of C/EBPβ[57, 65, 67]. As discussed above, steady-state granulopoiesis requires G-CSF signaling through C/EBPα. In EG, hyper-activation of G-CSFR causes a STAT3-dependent switch from C/EBPα to C/EBPβ[6, 58, 65, 68, 69]. This switch promotes the rapid proliferation, maturation, and subsequent release of neutrophils into the blood stream.

1.9 The Tissue Resident Macrophage Revolution

Macrophages are specialized immune cells capable of phagocytosing infectious agents and cell debris, secreting cytokines and inflammatory mediators, and antigen presentation[70]. Macrophage function and phenotype can vary greatly depending on its location within the body and activating stimulus[5, 70-74]. It has long been thought, that macrophages differentiate from bone marrow-derived monocytes, and that the cytokine cues present at the site of activation determined the macrophages function[75-77]. While there are bone marrow-derived circulating monocytes which do behave in this fashion, recent studies have clearly demonstrated that there are distinct populations of tissue resident macrophages (TRMs) that are capable of maintenance and self renewal independent of the bone marrow[5, 70, 72, 73, 77-80].

One of the first reports to demonstrate these findings was published by Schulz et al[78]. Their studies utilized a sophisticated cell lineage tracing system and bone marrow reconstitution to assess whether TRMs were dependent on the bone marrow. Their findings, summarized in Table 1.1, demonstrate that some pools of TRMs are maintained completely independent of the bone marrow[78]. Langerhans and Kupffer cells isolated from chimeric mice were 100% host-derived[78]. Splenic and pancreatic macrophages were found to be 90% host-derived and 10% donor-derived[78]. Alveolar and kidney macrophages were

found to be heterogeneous with 50% being donor-derived and 50% being host-derived[78]. These findings forced scientists to re-evaluate the interpretation of decades of findings regarding macrophage function in the pathogenesis of disease.

In addition to TRMs being independent of the bone marrow, many studies have shown that TRM populations are established during embryonic development. Langerhans cells, microglia, Kupffer cells, pancreatic macrophages, alveolar macrophages, and splenic red pulp macrophages are derived from the embryonic yolk sac[5, 70, 72, 75, 78-80]. It is worth noting that during embryonic development hematopoiesis occurs within the fetal liver, rather then in the bone marrow. During the transition period from fetal liver to bone marrow hematopoiesis, the remaining TRM populations are seeded into their respective tissues (Table 1.2)[5].

While many tissues have TRMs, some tissues do rely on the classic bone marrow-derived monocytes to infiltrate into the tissues and maintain immune surveillance. The gut is one example of a tissue that appears to rely exclusively on monocyte-derived macrophages to maintain normal function[30, 70, 71, 77, 81]. However, to date most tissues have been shown to maintain a TRM population that is responsible, at least in part, for normal function.

TRMs are specialized to help maintain proper function of diverse tissue types. However, under infectious or inflammatory conditions, bone marrow-derived $CD11c^{hi}$ monocyte-derived macrophages respond to chemotactic gradients and enter the inflamed or damaged tissues[30, 82, 83]. These inflammatory macrophages specialize in phagocytosing infectious agents and cellular debris and aid in priming the adaptive immune system to respond to chronic infections. During the resolution of inflammation, TRMs exert an anti-inflammatory effect, reducing the number of inflammatory macrophages infiltrating into the tissue[5, 83].

The discovery of TRM independence from the BM, has severely complicated our understanding of the regulation of granulopoiesis. One of the main questions researchers have asked is 'where are the majority of neutrophils being cleared to maintain steady state granulopoiesis?'. Now that several distinct populations of TRM have been shown to be independent and functionally distinct from each other and the bone marrow, it becomes more difficult to identify which populations of TRMs contribute to the clearance of apoptotic neutrophils and the regulation of granulopoiesis. Further research needs to be done to adequately address this question.

1.10 DSS-Induced Colitis

Inflammatory bowel disease (IBD) is a complex disease comprised of Crohn's disease and ulcerative colitis. In the developed world, these chronic inflammatory diseases of the intestine affect 1 out of 200 people[84]. Ulcerative colitis is characterized by loss of the intestinal mucosa starting at the rectum and extending continuously proximally. The destruction to the mucosa leaves an open mucosal wound or ulcer, allowing the bacterial microflora to establish opportunistic infections and maintain a chronic inflammatory state[48, 85]. Crohn's disease causes multifocal inflammation in non-continuous sections of the gastrointestinal tract. The inflammation in these lesions is transmural, affecting the entire thickness of the intestinal wall, causing significant fibrosis and thickening of the wall[48, 85]. As the disease progresses strictures can form and lead to obstructions of the bowel.

Due to the high incidence of IBD, lack of effective treatments, and the poor understanding of the pathogenesis of the disease, the use of animal models are needed to help identify the mechanisms underlying the pathogenesis of disease. Several animal models of colitis are currently used, however dextran sulphate sodium (DSS)-induced colitis is by far the most widely used[84-88]. This chemically-induced model of colitis is reproducible, simple to perform, and has histologic features that closely match those found in human UC [84-88].DSS is thought to be toxic to the

gut epithelial cells and disrupts the tight junctions between the epithelial cells in the mucosa. As gaps begin to form, bacterial products invade into the tissue and drive inflammation[48, 81, 84, 87, 88].

Initial colitis in this model is dependent on monocytes and granulocytes, as $Rag1^{-/-}$ mice that lack lymphocytes develop severe colitis[81, 86-89]. As the disease progresses the inflammatory innate immune cells invade into the mucosa and submucosa, causing the loss of crypts and eventually destruction of the entire epithelial layer[48, 85, 86]. In addition to the acute granulocyte-dependent colitis, recurring rounds of DSS administration followed by 14-28 days of water administration for recovery allow researchers to study the adaptive immune response in colitis as well as the mechanisms involved in crypt regeneration[44, 81, 90].

Studies have shown that the induction of colitis causes elevations in proinflammatory cytokines such as IL-1α, IL-1β, IL-6, IL-17, G-CSF, and MIP-1β[44, 48, 81, 85, 90-92]. These inflammatory mediators drive inflammation and help to induce the expression of chemokines such as Eotaxin and CCL2 that will enhance granulocyte recruitment to the inflamed colon.

1.11 Significance

Leukocyte trafficking plays a vital role in the immune system. The complex cell-cell interactions that mediate cellular adhesion, migration, and homing have been extensively studied. The role of selectins in leukocyte tethering and rolling during the process of trans-endothelial migration has been well characterized. $Fut^{-/-}$ mice lack functional selectin-ligand activity, and as expected have a mark selectin-dependent leukocyte trafficking deficiency. $Fut^{-/-}$ mice also have a leukocytosis primarily comprised of a neutrophilia. The mechanisms involved in the Fut-dependent neutrophilia are not known. Additionally, the effect of the loss of Fut4 and Fut7 activity on the immune response is unknown. Our studies seek to determine the underlying mechanisms responsible for the neutrophilia in $Fut^{-/-}$ mice, and to assess the role of α(1,3)-fucosylation on leukocytes on maintenance of homeostatic immunity and the pathogenesis mucosal injury. Bone marrow transplantation will be preformed to determine the relative contribution of bone marrow derived cells to maintaining the neutrophilia in Fut-/- mice. Assessment of transgenic mouse strains with myeloid specific expression or deletion of FUT7, enable us to determine the role of myeloid cell trafficking in regulating granulopoiesis. Additionally these mouse lines will be subjected to DSS-induced colitis to determine the effect the loss of Fut-dependent trafficking has on the pathogenesis of colitis.

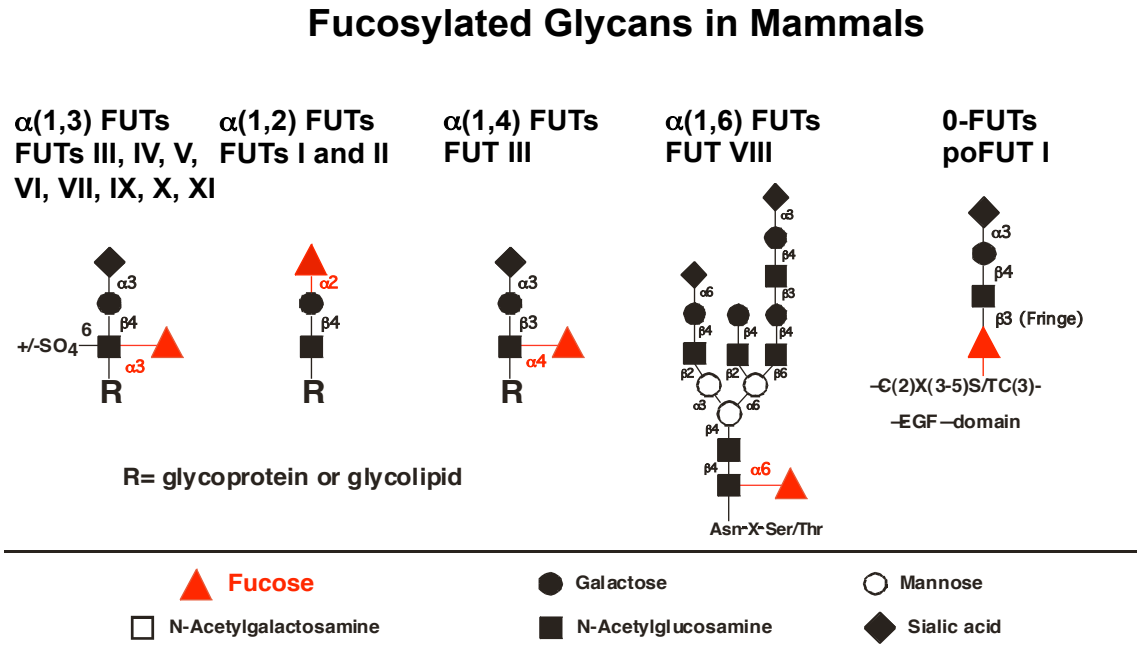

Figure 1.1 – Fucosyltransferases in Mammals

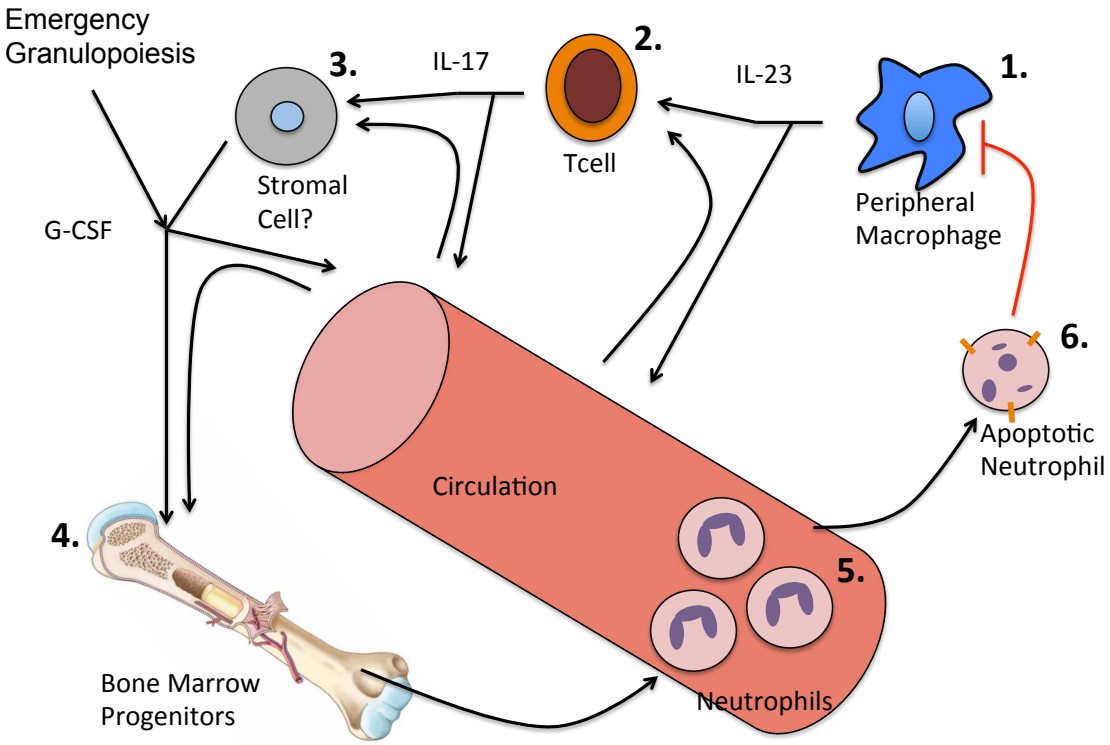

Figure 1.2 - Proposed Density-Dependent Feedback Loop that Regulates Granulopoiesis.
Macrophages and dendritic cells in peripheral tissues produce IL-23, which acts upon Tcells to produce IL-17, which causes G-CSF production. G-CSF stimulation of the BM increases the proliferation of granulocytic progenitor cells and drives the differentiation, maturation, and release of neutrophils into the vasculature. Neutrophils then exit the vasculature, undergo apoptosis and are taken up by peripheral phagocytes suppressing their production of IL-23 and decreasing granulocyte production.

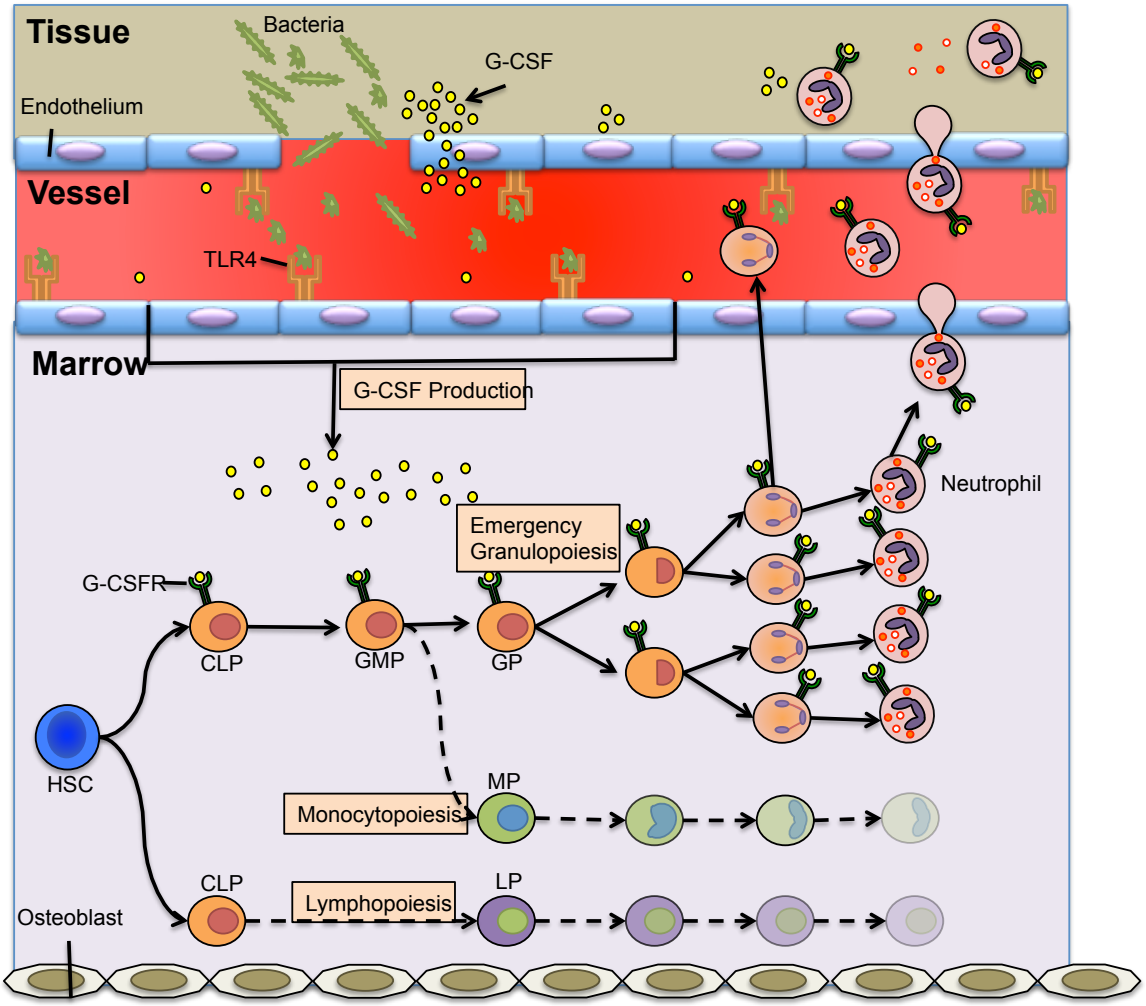

Figure 1.3 - Emergency Granulopoiesis
Under Infectious conditions bacterial products are recognized by Hematopoietic Stem Cells (HSCs) and non-hematopoietic cells such as endothelial cells. The recognition of bacterial products by TLR4 induces the production of high levels of G-CSF which promotes the proliferation of HSCs to create more neutrophils *de novo*. These neutrophils then mature and re released into the blood stream to combat infection. Activation of Emergency Granulopoiesis inhibits monocytopoiesis and lymphopoiesis.

Common Lymphoid Progenitors (CLPs), Granulocyte Monocyte Progenitors (GMPs), Granulocytes Progenitors (GPs), Monocyte Progenitors (MP), Lymphocyte Progenitors (LP)

	% Host-Derived	% Donor-Derived
Skin	100	0
Liver	99	1
Spleen	90	10
Pancreas	91	9
Lung	45	55
Kidney	44	56

Table 1.1 - TRM independence from the Bone Marrow
These results show the percentage of F4/80^{+} cells isolated from the organs of Bone Marrow Transplant mice were host derived or donor derived.

Tissue	Cell Type	Function
Adipose Tissue	Adipose-associated macrophages	Control Insulin Sensitivity and thermogenesis.
Blood	Ly-6C^{lo} monocytes	Intra-vascular TRM, clear endothelial cell debris.
Bone	Osteoclasts	Resorb bone by disrupting matrix.
	Bone Marrow Macrophages	Support hematopoiesis and maintain stem cells in their niches. Self-renewing population.
Central Nervous System	Microglia	Protect neurons, remove cellular debris, maintain immune surveillance. Derived from embryonic yolk-sac and maintained independent of BM.
Gastrointestinal Tract	Intestinal Macrophages	Blood monocyte derived, maintain intestinal homeostasis and modulate immune response to commensal bacteria.
Liver	Kupffer Cells	Maintained independently from BM. Clear cell debris and infectious material from blood.
Lung	Alveolar Macrophage	Clearance of inhaled pathogens and debris.
Skin	Langerhans Cells	Present antigens to Tcells, yolk-sac derived. Maintained independently from BM.
Spleen	Red Pulp Macrophages	Clear erythrocytes and metabolize iron. Yolk-sac derived, maintained independent of BM.

Table 1.2 - Locations and known functions of TRMs. Adopted from Davies et al.[5]

Chapter 2 – Methods and Protocols

2.1 Mice

All mice were maintained in a specific pathogen free environment. Mice were housed in standard shoebox cages, with constant access to chow and water. All experiments were approved by the Institutional Animal Care and Use Committee (IACUC) at the University of North Carolina-Chapel Hill. Animals had full access to husbandry and veterinary provided by DLAM. In compliance with ethical standards, the fewest number of mice necessary were used for experiments. Experimental protocols minimized animal pain and distress.

All mouse lines are on the C57bl/6J genetic background. Fut4$^{-/-}$, Fut7$^{-/-}$, and Fut$^{-/-}$ mice were a gift from Dr. Lowe (University of Michigan) and have been propagated and maintained at our facility. WT and Rag1$^{-/-}$ mice were purchased from The Jackson Laboratory and bred in-house for experimental use. To generate Rag1$^{-/-}$/Fut$^{-/-}$ mice, Rag1$^{-/-}$ males were bred to Fut$^{-/-}$ females, progeny were then genotyped and crossed until the triple null Rag1$^{-/-}$/Fut$^{-/-}$ mouse was obtained. These mice were then bred and maintained as homozygous null for Rag1, Fut4, and Fut7. ELP$^{-/-}$ and L-selectin$^{-/-}$ mice were a gift from Dr. Richard Hynes (MIT), and were

bred in-house for experimental use. P- and E-Selectin$^{-/-}$ mice were a gift from Dr. Claire Doerschuk (UNC), and were provided as needed for experiments.

2.2 Euthanasia

Mice were euthanized by asphyxiation in a CO_2 chamber and death was ensured by cervical dislocation, exsanguination or lethal tissue harvest, in compliance with IACUC and DLAM regulations

2.3 Tissue Isolation

After euthanasia animals were wetted with 70% ethanol to minimize bacterial contamination of isolated tissues. Thoracotomy or laparotomy was performed, and the required organs (spleen, liver, lungs, colon, lymph nodes, heart) were harvested.

2.4 Blood Collection

After euthanasia, the peritoneal cavity was opened and the intestines were reflected to the side, exposing the inferior vena cava. Blood was withdrawn from the IVC using a 25-gauge needle fitted to a 1ml syringe filled with 70ul sodium citrate solution (Sigma) to prevent clotting. Each adult mouse yielded 500-800ul of blood.

2.5 Complete Blood Counts

Complete Blood Counts (CBC) were determined in venous whole blood treated with EDTA, using an automated Heska Veterainry hematology analyzer, and appropriate species-specific software and parameters. The automated cell counter provides the total leukocyte, granulocyte, monocyte, lymphocyte, hematocrit, and platelet counts for each sample. Samples from animals were run in duplicate to ensure accuracy.

2.6 Red Blood Cell Lysis

Red blood cell (RBC) lysis was performed using BD Pharm Lyse buffer according to manufacturer's specifications. In brief, the buffer is diluted into DI water 1:10 and incubated with blood sample (2 ml buffer for every 500 ul whole blood) for 10 minutes in the dark at room temperature, to lyse the RBCs. The cells are then centrifuged at 300 x g for 5 min and resuspended in PBS. This protocol was repeated if necessary.

2.7 Plasma Isolation

Whole venous blood was collected as described above using sodium citrate as an anti-coagulant. Samples were centrifuged for 20 min at 300 x g with no brake. The red cells pellet, and the leukocytes form a buffy

coat at the interface between RBC pellet and the plasma supernatant. The plasma was then carefully isolated with a pipette, avoiding the buffy coat. The samples were placed in labeled tubes and used directly for experiments or frozen at -80°C for subsequent analysis.

2.8 Bio-Plex Cytokine Analysis

Circulating cytokine levels were quantitated using a 23-plex cytokine array (BIO-RAD). Plasma was isolated as described above from untreated and LPS-injected WT and $Fut^{-/-}$ mice, and used immediately for the assay. The assay was performed by the Advanced Analytics Core at UNC-CH according to the manufacturers instructions. The assay plate was washed, 50 ul of pre-mixed beads were added to the wells, and the wells were washed 2x. 50 ul of samples, standards, or blanks were added to the beads in the well, and incubated shaking (850 rpm) overnight at room temperature. The wells were then washed 3x, 25 ul of detection antibody was added to each well and incubated for 30 minutes at RT. Beads were then washed 3x, resuspended in 125 ul assay buffer and analyzed on a MAGPIX plate reader. Florescence was measured and compared to the standard curve to determine the concentration of each cytokine in each sample.

2.9 IL-23 ELISA

IL-23 production by macrophage cultures was determined using an IL-23 Quantikine ELISA (R&D) according to manufacturers protocol. Supernatants were isolated from macrophage cultures, spun at 300 x g for 5 min to pellet cells and debris, and frozen at -80°C until the ELISA was performed. The ELISA plate was blocked with assay diluent for 1 hour at RT. 50ul of samples or standards were then incubated in the assay plate wells for 4 hours at RT. The plate was washed 5x with wash buffer and incubated with 100uL of IL-23 antibody conjugate for 2 hours at RT. The plate was washed 5x, then incubated with 100uL substrate solution for 30 min at RT in the dark. The reaction was stopped with 100uL stop solution and the absorbance was determined at 450nm. Results were compared to a generated standard curve to determine the IL-23 concentration in each sample. Samples were run in triplicate.

2.10 Mononuclear Cell Isolation

Histopaque-1077 (Sigma) was used to isolate mononuclear cells from a cell suspension by density gradient centrifugation. Histopaque-1077 was carefully layered under the cell suspension, and centrifuged at 300 x g for 30 minutes at RT with no brake. After centrifugation the mononuclear cells are recovered from the gradient interface and

transferred to a new tube, resuspended with fresh media and washed 3x, then centrifuged for 5 minutes a 300 x g at 4°C and used in experiments.

2.11 In Vitro Stimulation of Leukocyte Activation

Mononuclear cells from the spleen, bone marrow, blood or other tissues were isolated as described above and resuspended in RPMI with 10% FBS and Penicillin/Streptomycin. $1x10^6$ purified cells in 5ml media were then incubated with 10ul PMA/Ionomycin with Brefeldin A (BD) or in untreated culture media for 4 hours. PMA/Ionomycin activates leukocytes to induce cytokine production, and Brefeldin A inhibits vesicle transport to ensure that produced cytokines are not secreted. After stimulation the cells are washed 3x by centrifugation at 300 x g for 5 min at 4°C, and resuspended in fresh culture media for analysis by flow cytometry.

2.12 Flow Cytometry

Flow cytometry was used to rapidly identify cell populations and assess cytokine production. $1x10^6$ unstimulated or stimulated (as described above) cells were plated into each well of a 96-well plate and washed 3x by centrifuging at 300 x g and resuspending the cells in Facs buffer (1x PBS, .5% BSA, 2 mM EDTA). The cells were then incubated with 100 ul surface staining antibody cocktail (antibodies each at 1 ug/mL) containing the desired cell linage-specific antibodies for 30 min at

4°C, protected from light. Cells were then washed 3x as described above. For intracellular cytokine (IC) staining, cells were fixed with 100 uL fixation buffer (Biolegend) for 20 minutes in the dark, permeabilized by incubation with 100 uL perm/wash buffer (Biolegend) for 5 minutes, washed 3x by centrifuging the plate at 300 x g for 5 minutes, and then resuspending the cells in perm/wash buffer. Cells were then incubated with 50 ul of IC antibody cocktail in perm/wash buffer (antibodies at 2ug/mL) for 1 hour at 4°C, washed 3x, resuspended in Facs buffer, transferred to clean assay tubes, and analyzed using a Cyan Flow Cytometer (DAKO).

2.13 Messenger RNA Isolation

Qiagen RNeasy kits were used to isolate mRNA from cultured cells or freshly harvested cells isolated from tissues. $5x10^6$ cells were suspended in 600 ul RLT buffer and pipetted into a Qiashredder column and centrifuged at max speed for 2 min. The cell lysates were then mixed with 600ul 70% ethanol, transferred to an mRNA isolation column, and spun at 9000 rpm for 20 seconds. The flow through was discarded, and the column was washed once with RW1 buffer, and twice with RPE buffer. The membrane was dried by spinning at max speed for 1 minute. mRNA was then eluted from the column with 50ul nuclease-free water.

mRNA concentrations were assessed using a nano-drop spectrophotometer, then stored at -80°C.

2.14 cDNA Synthesis

mRNA was converted to cDNA using the SuperScriptase III kit (Invitrogen), according to the manufacturers protocol. To convert 24 ul of mRNA to cDNA a primary mix was made by combining the 24 ul mRNA, 3 ul dNTPs, 1.5 ul of oligo dTs, and 6 ul H2O. The mix was heated to 65°C for 5 minutes followed by 4°C for at least 2 minutes. A secondary mix of 6 ul buffer, 6 ul DTT, 12 ul MgCl, 1.5ul superscriptatse, 1.5 ul RNaseout was added, and the reaction was heated at 50°C for 50 minutes followed by 85°C for 5 min. To degrade the mRNA, 1.5 ul RNaseH was added and incubated at 37°C for 20 minutes. After the reaction the cDNA was diluted to 5 ng/uL and stored at -20°C.

2.15 Quantitative Polymerase Chain Reaction

To assess gene transcription, quantitative polymerase chain reaction (qPCR) was performed on cDNA samples prepared as described above. Primers and probes for murine IL-23p19, IL-6, β-actin, fibrinogen, and IL-10 were purchased from Applied Biosystems. A 20 ul reaction was used, containing 10 ul of Taqman universal mastermix II (ABI), 1 ul primer/probe, 4 ul cDNA (20ng), 5 ul H2O. The reaction was run on an

ABI 7500 Fast machine. The ΔΔCT method was used to determine alterations in gene transcription between experimental groups, using β-actin as the housekeeping gene.

2.16 CD4 Tcell Isolation

Dynabeads Untouched CD4 Mouse Tcell isolation kit (Invitrogen) was used to isolate Tcells from freshly isolated splenocytes. Beads were resuspended and 1 mL suspensions was added to tubes and placed onto the magnet for 1 minute to prewash. The supernatant was discarded, the tube was removed from magnet, and the beads were resuspended in 1 mL of isolation buffer. Splenocytes were diluted to $1x10^8$ cells per mL in isolation buffer, then 500 uL cell suspension was added to a clean tube containing 100 ul FBS and 100 ul antibody mixture for 20 minutes at 4°C. Cells were washed by adding 10 mL isolation buffer, then centrifuged at 300 x g for 5 minutes at 4°C. The cells were resuspended in 4 ml isolation buffer, and 1 mL prewashed beads were added and allowed to incubate for 20 minutes at RT. Five mL isolation buffer was added and the solution was mixed to resuspended cells and beads. One mL of the suspension is transferred to a new tube on the magnet for 2 minutes. Supernatant containing negatively isolated CD4 Tcells is collected in a new tube. The purity of the isolated cell suspension is confirmed by staining with CD4, and assessing percentage of $CD4^+$ cells via flow

cytometry as described above. The sample purity was confirmed to be >90%.

2.17 In Vitro Th17 Differentiation

Naïve CD4+ Tcells were subjected to an in vitro differentiation protocol first described by Ivanov et al. [47]. Tcells were plated into a 12-well plate in RPMI medium with 10% FBS, pen/strep, α-CD28 (1 ug/mL), α-CD3 (0.25 ug/mL), IL-23 (10 ng/mL), IL-6 (20 ng/mL), and TGFβ (0.3 ng/mL) for 7 days at 37°C. After differentiation, Tcells were stimulated with PMA/Ionomycin and assessed for IL-17 production via Flow cytometry as described above.

2.18 Neutrophil Depletion

Eight to twelve week old male WT or $Fut^{-/-}$ mice were administered the neutrophil-specific Ly-6g (1A8) antibody (i.p.) to deplete circulating neutrophils. WT mice received 1mg of antibody, $Fut^{-/-}$ mice were given 1 mg, 9 mg, or an equal volume of PBS as control. Blood samples were taken at 0, 12, 24, and 36 hours post injection and circulating neutrophil counts were assessed as described above.

2.19 In Vivo Endotoxemia

Eight to ten week old male WT or $Fut^{-/-}$ mice were injected i.p. with 1 mg/kg of LPS (Sigma) in PBS. Venous blood samples were obtained at 0, 12, 24, 36, and 48 hours post injection and circulating neutrophil counts were assessed as described above.

2.20 Bone Marrow Isolation

Bone marrow (BM) was isolated from the femur and tibia of 12 week-old male mice. Mice were euthanized and the femurs and tibias were harvested. A 25-gauge needle attached to a 20 mL syringe filled with chilled RPMI was inserted into the end of the bone and the marrow was flushed out into a sterile pyrogen-free 50 ml conical tube. A wide mouth pipette was then used to break up the clumps of cells. The cells were then spun at 300 x g for 5 min at 4°C and resuspended in fresh media for subsequent experimental use.

2.21 Irradiation

Six to eight week old male WT or $Fut^{-/-}$ were placed in a rodent irradiation pie container and irradiated with 9 gy or 12 gy of ionizing radiation in a XRAD 320 biological irradiator. The mice were then transferred to sterile cages and given acidified water (pH 2.7) ad libitum

for 14 days. Mouse weight and general health was monitored and recorded daily.

2.22 Bone Marrow Transplant

WT or $Fut^{-/-}$ mice were irradiated as described above, and allowed to recover for 4 hours, during which time BM was isolated from WT or $Fut^{-/-}$ mice. Irradiated mice were anesthetized with isoflourine, and injected i.v. via the tail vein with $1x10^7$ BM cells from either WT or $Fut^{-/-}$ mice. The injected mice were returned to sterile cages and given acidified water for 2 weeks. Six weeks after transplant, the mice were euthanized, venous blood was harvested for CBC, and splenocytes were assessed for IL-17 production via flow cytometry as previously described.

2.23 Peripheral Blood Neutrophil Isolation

Neutrophils were isolated from the venous blood of WT or $Fut^{-/-}$ mice as described above. RBC's were lysed as described above. The remaining cell suspension was layered over histopaque-1077 and centrifuged at 300 x g for 30 minutes. The neutrophil-enriched cell pellet was washed in Facs buffer, and pelleted again. The neutrophils were then resuspended in RPMI with 10% FBS. Flow cytometry was used to assess purity using a Ly-6G antibody. Purity normally ranged from 75-85%.

2.24 Neutrophil Fluorescent Labeling

Isolated neutrophils were transferred into serum free RPMI media containing 5 uM CellTracker Dye (CMFDA or CMPTX) (Invitrogen) for 45 minutes at 37°C to uptake the dye. The neutrophils were then centrifuged at 300 x g for 5 min, resuspended in fresh pre-warmed media for 30 minutes, washed in RPMI with 10% FBS, and used in experiments. Fluorescent labeling is confirmed by florescence microscopy.

2.25 Adoptive Neutrophil Transfer

Fluorescent-labeled neutrophils were suspended in Facs buffer at $1x10^7$ cells/mL. 100 uL of neutrophils were injected i.v. into WT or $Fut^{-/-}$ mice. Mice were sacrificed 24-hours post injection, blood was drawn for CBC, and spleen and liver were harvested to assess neutrophil accumulation in those organs. The spleen was disassociated in Facs buffer using frosted slides. The cell suspension was then passed through a cell strainer and maintained at 4°C. The liver was minced with sharp scissors and incubated in RPMI containing collagenase dispase (Roche) for 30 minutes at 37°C. The residual tissue was minced further with a razor blade and subjected to another 20 minutes of digestion. The suspension was passed through a 50 um cell strainer to remove debris. Cell suspensions from spleen and liver were then stained with α-Ly-6G, α-F4/80, and α-CD45 as described above, and analyzed via flow cytometry.

2.26 Primary Kupffer Cell Isolation

Ten to twelve week old male WT or $Fut^{-/-}$ mice were euthanized, a laparotomy was performed, and the IVC was cannulated with a 25-gauge butterfly needle. A perfusion pump was used to infuse perfusion buffer (1x HBSS, 2 mM Hepes, 5 mM EGTA; 3 mL/min)[93, 94]. The hepatic portal vein was incised to allow full perfusion. The liver was infused until pale yellow in color (45 mL of perfusion buffer), then 50 ml pre-warmed digestion solution (1xHBSS, 1.25mg Liberase TM) was infused at a rate of 3 mL/min. The liver was carefully removed, and disassociated in DMEM with 10% FBS. The resulting cell suspension contains kupffer cells and the larger hepatocytes. The cell suspension was centrifuged at 50 g for 2 min to pellet the hepatocytes leaving the kupffer cells in suspension[93, 94]. The Kupffer cells in the supernatant were pelleted at 300 x g for 5 min. Isolation purity was assessed via flow cytometric analysis of $F4/80^{+}$ cells, and was usually >80%.

2.27 Bone Marrow Derived Macrophage (BM-MC) and Dendritic Cell (BM-DC) In Vitro Differentiation

BM was isolated as described above. BM was suspended in RPMI with 10% FBS and Pen/Strep in a T75 culture flask for 1 hour. This allowed mature cells to adhere to the plastic. After an hour the non-

adherent cells were isolated, pelleted at 300 x g for 5 min, resuspended in RPMI with 10% FBS,Pen/strep,10 ng/mL M-CSF (for BM-MCs) or 20 ng/mL GM-CSF (for BM-DCs), and plated in T75 culture flasks at 37°C [20, 27, 28, 46]. After 3 days, 20 mL fresh media was added to both cultures. After 5 days media was removed from BM-MC cultures and replaced with fresh differentiation media. After 7 days both cultures had adherent differentiated phagocytes. Cells were removed from culture flasks by incubation with trypsin and re-plated into experimental plates. Differentiation was confirmed by flow cytometry for $CD11B^+$ (MC) or $CD11C^+$(DCs).

2.28 In Vitro Phagocytic Rate Assay

$1x10^5$ BM-MC, BM-DC, or primary Kupffer cells (pKCs) were plated in a 96-well plate and allowed to adhere for 1 hour at 37°C. Labeled neutrophils were prepared as described above, and incubated at 50°C for 30 minutes followed by 2 hours at 37°C to induce apoptosis. $1x10^6$ apoptotic neutrophils were added to each well containing the phagocytes and incubated for 1 hour. Wells were then gently washed to remove un-engulfed neutrophils. Phagocytes were harvested with trypsin, washed in RPMI, stained with α-Ly-6G, and assessed via flow cytometry. Phagocytes that had ingested a labeled neutrophil were $Ly\text{-}6G^-CMFDA^+$. The

percentage of each culture that was positive for ingesting at least one neutrophil were calculated, and reported as phagocytic rate.

2.29 In Vitro Efferocytosis assay

$1x10^5$ BM-MC, BM-DC, or pKCs were plated in a 96-well plate and allowed to adhere for 1 hour at 37°C. Neutrophils were isolated, labeled, and apoptosis was induced as described above. Adherent phagocytes were incubated in control media or stimulated with 10ng/mL LPS in RPMI with 10% FBS for 4 hours to induce IL-23 production, then incubated with $1x10^6$ apoptotic neutrophils for 2 hours[17, 27, 34, 35]. Supernatants were collected to measure IL-23 production via ELISA, and adherent cells were lysed with RLT buffer, and mRNA was isolated as described above.

2.30 DSS-Induced Colitis

Colitis severity has been shown to be strongly influenced by the microflora. Therefore, because littermate controls are not available for the $Fut^{-/-}$, $Rag1^{-/-}$, or $Rag1^{-/-}/Fut^{-/-}$ strains, bedding from experimental mice was mixed for 7 days before the start of the experiment. Colitis was induced by administering 3% DSS in the drinking water of experimental mice. Mice were given fresh DSS or control water every day for 5 days followed by regular water for 0, 3, or 5 days. Mouse weight and fecal occult bleeding status were monitored daily.

2.31 Preparation of Colon for Histology

Following euthanasia, the colon was removed, flushed with cold PBS to remove fecal material, and opened longitudinally. The colon was then placed between two pieces of moistened bibulous paper that are fastened closed with paper clips, and then fixed in phosphate buffered formalin overnight at 4°C. The tissue was then equilibrated into a 10% sucrose solution for 24 hours and 30% sucrose solution for another 24 hours. It was then cut into proximal, middle, and distal thirds, embedded individually into OCT freezing compound, and frozen on dry ice. 7 μm sections were cut from the tissue block and mounted on slides and allowed to dry overnight at RT.

2.32 Hematoxylin and Eosin (H&E) Staining of Tissue Sections

Dried slides were placed in distilled water for 3 minutes, and stained with Meyers Hematoxylin for 3 minutes. The slides were then washed in distilled water for 5 minutes, dipped in .3% hydrochloric acid in ethanol, stained in eosin for 30 seconds, and washed in distilled water for 5 minutes. The slides were dehydrated in increasing concentrations of ethanol (70% for 2 minutes, 95% for 2 minutes 100% for 2 minutes, and xylenes for 5 minutes), cover-slipped with cytoseal, and allowed to dry for 1 hour before imaging.

2.33 Histologic Scoring of Colon Sections

H&E stained sections were imaged consecutively starting at the rectum and continuing proximally to the mid-colon. Each image was scored for disease severity, and all scores are averaged to determine the final histologic score for the animal. Three criteria are scored: inflammation severity, inflammation extent, and crypt damage[95]. Each category were scored 0 (no disease/change) to 4 (extremely severe). Inflammation severity (P1) scores were: 0-No inflammation present, 1-Mild inflammation, 2-Moderate inflammation, 3-Severe inflammation. Inflammation extent (P2) was scored as: 0- None, 1-Mucosa only, 2-Submucosa and mucosa, 3-Transmural. Crypt damage (P3) was scored as: 0-No change, 1- Crypts are 1/3 above muscularis mucosa (mm), 2-Crypts are 2/3 above the mm, 3- Crypts absent but epithelium intact, 4-Crypts absent and epithelium gone. If disease severity varies across the image the two sections can be scored independently, and the percent involvement can be divided between the divergent severities. The percent involvement (I) was scored as: 0-None, 1-25%, 2-50%, 3-75%, 4-100% of the mucosa in the image. The scores were then calculated as follows (P1xI)+(P2xI)+(P3xI)= Histologic score[95].

2.34 Statistical Analysis

For two group comparisons, paired two-tailed Student T-Tests were performed. A p value of less than 0.05 was considered significant. For multiple group comparisons an anova was performed with a Tukeys multiple comparison post-hoc test. A p value of less than 0.05 was considered significant. Survival curve significance was determined using a Chi square test with p values of less than 0.05 was considered significant. Graphing and statistical analysis was performed using Graphpad Prism v6.0e software.

Chapter 3 – Results

3.1) Characterization of the Immune Response in Fut$^{-/-}$ Mice.

3.1.1 Leukocyte Counts

Fut$^{-/-}$ mice have been previously shown to have a pronounced selectin-dependent leukocyte trafficking deficiency. By performing a complete blood count (CBC), we confirmed reports that Fut$^{-/-}$ mice have a leukocytosis (Figure 3.1), comprised of a 12-fold increase in neutrophils, 4-fold increase in monocytes, and a 1.4-fold increase in lymphocytes in circulation compared to WT mice. These results suggest that in addition to a leukocyte trafficking deficiency, Fut$^{-/-}$ mice may have altered hematopoiesis.

Because Fut$^{-/-}$ mice lack both functional Fut4 and Fut7 we sought to determine each enzyme's contribution to the leukocytosis found in Fut$^{-/-}$ mice. Whole blood CBCs were done on Fut4$^{-/-}$ and Fut7$^{-/-}$ animals and compared to WT and Fut$^{-/-}$ mice. As shown in figure 3.1, Fut4$^{-/-}$ animals had near WT levels of neutrophils, monocytes, and lymphocytes, while Fut7$^{-/-}$ animals had elevated leukocyte counts compared to WT mice. The leukocytosis in Fut7$^{-/-}$ mice was 20% lower then Fut$^{-/-}$ mice. These results show that when Fut4 is lost, Fut7 is able to almost completely

compensate so that only a minimal phenotype is observed. In contrast when Fut7 is lost, Fut4 can only provide minimal compensation, and a significant leukocytosis is observed. This clearly demonstrates that Fut7 is primarily responsible for fucosylating the glycoproteins responsible for the leukocytosis observed in $Fut^{-/-}$ mice.

3.1.2 Fut-Dependent Alterations of Circulating Cytokine Levels

We hypothesized that the circulating cytokine profile would be altered in $Fut^{-/-}$ mice compared to WT mice due to the increase in circulating leukocyte counts and the associated trafficking and homing defects. To assess the immunologic state of the mice, we performed a bio-plex multi-analyte cytokine array to measure any Fut-dependent alterations in circulating cytokine concentrations. We measured the concentrations of Interleukin-1α, -1β, -2, -3, -4, -5, -6, -9, -10, -12(p40), -12(p70), -13, -17, Eotaxin, G-CSF, GM-CSF, IFNγ, KC, MCP-1, MIP-1α, MIP-1β, RANTES, and TNFα in WT and $Fut^{-/-}$ plasma (Table 3.1). Table (3.2), shows a summary of significant changes observed in untreated $Fut^{-/-}$ mice. We observed significant increases in IL-13, IL-17, G-CSF, MCP-1, and MIP-1α. Of special note are the increases in IL-17 (2.5-fold) and G-CSF (5.5-fold) as these factors are thought to play a crucial role in the regulation of granulopoiesis.

We also sought to determine the responsiveness of the immune system in $Fut^{-/-}$ mice to infectious stimuli (LPS). We stimulated WT and $Fut^{-/-}$ mice with LPS (1mg/kg i.p.), and measured plasma cytokine concentrations 12 hours post injection using the same bio-plex assay described above. As shown in Table 3.3, IL-1α, IL-1β, IL-6, IL-10, IL-17, and G-CSF concentrations were elevated compared to WT LPS treated mice. In contrast, Eotaxin, MCP-1, MIP-1β, and TNFα concentrations were decreased compared to WT LPS treated mice. These results show that Fut-/- mice can still initiate an inflammatory response to LPS, however it is characterized by the production of more inflammatory cytokines and fewer chemotactic factors then WT mice.

Results from the bio-plex cytokine assay and the CBCs taken together offer interesting insights into the regulation of the immune response. $Fut^{-/-}$ mice have a 4-fold increase in circulating monocytes and elevated concentrations of the macrophage chemotactic factors MCP-1 (CCL2) and MIP-1α (CCL3) which should promote monocyte migration into tissues. Despite the monocytosis in unstimulated $Fut^{-/-}$ mice, circulating plasma concentrations of IL-6 and IL-10 (both of which are produced by monocytes in copious amounts) were not different from WT concentrations. Following LPS stimulation, Eotaxin, CCL2, and CCL3 fail to be produced at WT levels, however proinflammatory cytokine IL-6 and anti-inflammatory cytokine IL-10 concentrations are significantly

elevated. These data suggest that there may be an unknown regulatory mechanism limiting circulating monocyte cytokine production in unstimulated mice, which is overcome by LPS activation. Additionally, the enhanced production of IL-17 and G-CSF in both stimulated and unstimulated mice shows that there is increased granulopoietic signaling stimuli in $Fut^{-/-}$ mice, which may be at least partially responsible for the observed neutrophilia.

3.1.3 Expansion of IL-17-Producing Leukocyte Populations in Fut-/- Mice

Interleukin-17 is a proinflammatory cytokine that has been implicated in the pathogenesis of autoimmune diseases (multiple sclerosis, lupus, etc), immune response to helminth infection, allergy (asthma), and even cardiovascular disease (atherosclerosis). Due to the pleiotropic contribution of IL-17 to the pathogenesis of disease, we sought to identify the mechanism of enhanced IL-17 production in $Fut^{-/-}$ mice. Flow cytometry was used to analyze, IL-17 production in single cell suspensions of mononuclear leukocytes isolated from blood, spleen, or lymph nodes of WT or $Fut^{-/-}$ mice. Mononuclear cells were stimulated with PMA/Ionomycin and Brefeldin A for 4 hours, fixed/permeabilized, and stained for surface markers of cell lineage, and for intracellular IL-17. Figure 3.2A shows a representative histogram of IL-17 staining of WT and $Fut^{-/-}$ mononuclear splenocytes. We identified a 19-fold increase in the

number of IL-17-producing $CD45^+$ mononuclear splenocytes in $Fut^{-/-}$ mice compared to WT mice. Further analysis (Figure 3.2B) revealed a 10-fold increase in Th17 cells ($CD3^+CD4^+IL\text{-}17^+$), a 23-fold increase in Natural Killer Tcells (NKT;$CD3^+DX5^+CD1d^+IL\text{-}17^+$), a 18-fold increase in γδ Tcells ($CD3^+CD4^-\gamma\delta TCR^+$ $IL\text{-}17^+$), and a 24-fold increase in Innate Lymphoid Cells (ILC;$CD3^-CD4^-CD8^-Nk1.1^-B220^-\gamma\delta TCR^-CD45^+IL\text{-}17^+$) compared to WT mice. These results show a marked expansion of IL-17-producing cell types in $Fut^{-/-}$ mice.

It is unclear the activity of which fucosyltransferase is primarily associated with the regulating IL-17 production. To determine if the expansion of IL-17-producing cells was dependent on the activity of Fut4 or Fut7, we analyzed the number of IL-17-producing cells in the spleen of $Fut4^{-/-}$ or $Fut7^{-/-}$ mice. As seen in Figure 3.2B, we determined that the loss of Fut4 activity only slightly increased the number of IL-17-producing cells (Th17 1.2 fold, NKT 2-fold, γδ Tcell 3-fold, ILC 2.5-fold). In contrast, the loss $Fut7^{-/-}$ activity resulted in a marked expansion of IL-17-producing cells (Th17 7.5-fold, NKT 19-fold, γδ Tcells 15-fold, ILC 20-fold) compared to WT mice. Similar to the CBC data, these data show that processes primarily dependent on Fut7 activity are largely responsible for the expansion of IL-17-producing cell populations.

Based on these data we hypothesized that the loss of Fut4 and Fut7 activity enhanced IL-17 production as the result of altered intracellular

signaling within the IL-17-producing leukocytes. We isolated mRNA from WT, Fut4$^{-/-}$, Fut7$^{-/-}$, and Fut$^{-/-}$ splenocytes, converted it to cDNA, and ran quantitative polymerase chain reactions (qPCR) to assess gene transcription of IL-17, RORγt, and IL-23. We found a significant increase in IL-17 gene transcription in Fut7$^{-/-}$ (17-fold) and Fut$^{-/-}$ (28-fold) mice compared to WT and Fut4$^{-/-}$ mice (Figure 3.3A). RORγt levels were also elevated in Fut7$^{-/-}$ (6-fold) and Fut$^{-/-}$ (9-fold) mice compared to WT and Fut4$^{-/-}$ mice. Interestingly IL-23 gene expression levels were not significantly different among the genotypes tested.

Together these results suggest an increase in the signaling for IL-17 production. However, the changes in mRNA production were similar to the changes in cell number we observed. Thus it is possible that the changes in gene expression reflect only the increased IL-17-producing cell population sizes. Therefore, we performed an in vitro Tcell differentiation assay. We isolated naïve CD4 Tcells from WT and Fut$^{-/-}$ mice with 95% purity by negatively selecting CD4 Tcells using magnetic beads. The naïve Tcells were then incubated for five days with IL-23, TGFβ, and IL-6 to differentiate the cells into a Th17 phenotype. At the end of the five day incubation period, the Tcells were harvested, stimulated with PMA/Ion with Brefeldin A, and stained for intracellular IL-17. Figure 3.3B, shows that under controlled in vitro conditions an equal percentage of Tcells became Th17 cells from WT and Fut$^{-/-}$ mice. These results

demonstrated that in vitro the signaling and differentiation pathways for IL-17 producing Tcells were not altered by the loss of FUT4 and FUT7. This suggests that in vivo the increased prevalence of IL-17 producing cells in $Fut^{-/-}$ mice is not the result altered Th17 differentiation, but rather an increase in polarizing conditions such as IL-23, TGFβ, and IL-6. Together these results suggest that the intracellular signaling pathways regulating the production of IL-17 are unaltered in $Fut^{-/-}$ mice. We therefore hypothesized that the increase in IL-17 production and IL-17-producing cell populations were related to the leukocyte trafficking deficiency.

3.1.4 Fut-Dependent IL-17 expansion and Neutrophilia are Selectin-Dependent

Fut4 and Fut7 are known to fucosylate the selectin ligands. However, it is reasonable to consider that they may fucosylate additional glycoproteins that express similar underlying glycan structures, especially Fut4 that is expressed in a wider variety of cell types. Experiments were performed to determine whether the leukocytosis and cytokine alterations required Fut-dependent selectin ligand activity. To test our hypothesis that the leukocytosis and IL-17 phenotypes resulted from the loss of selectin-dependent trafficking we performed CBCs and flow cytometric analysis of IL-17-producing cell populations in WT, $Fut^{-/-}$, P-selectin

Glycoprotein Ligand-1 (PSGL-1) $^{-/-}$, P-selectin$^{-/-}$, E-selectin$^{-/-}$, L-selectin$^{-/-}$, or ELP-selectin$^{-/-}$ mice. Results from the individual selectin-deficient mice can be compared to the results Fut$^{-/-}$ and ELP$^{-/-}$ mice to determine which, if any, of the selectins contribute to the leukocytosis and IL-17 phenotypes. As shown in Figure 3.4A, PSGL-1$^{-/-}$, P-sel$^{-/-}$, E-sel$^{-/-}$, and L-sel$^{-/-}$ mice all had normal circulating leukocyte counts. The ELP$^{-/-}$ mice however, completely recapitulated the leukocytosis observed in Fut$^{-/-}$ mice, including the 12-fold increase in granulocytes, 4-fold increase in monocytes, and a 1.4-fold increase in lymphocytes. These results show that the leukocytosis observed in Fut$^{-/-}$ mice is selectin dependent.

Analysis of the IL-17-producing cell populations in the selectin-deficient mice showed findings similar to the results of the leukocyte counts. PSGL-1$^{-/-}$, P-sel$^{-/-}$, E-Sel$^{-/-}$, and L-sel$^{-/-}$ mice had IL-17-producing cell counts of Th17, NKT, $\gamma\delta$ Tcells, and ILCs that were similar to counts in WT mice. The cell counts in ELP$^{-/-}$ mice however, recapitulated the expansions of Th17, NKT, $\gamma\delta$ Tcells and ILC populations seen in Fut$^{-/-}$ mice (Figure 3.4B).

These experiments strongly suggest that the expansion of IL-17-producing cells and the neutrophilia observed in Fut$^{-/-}$ mice is dependent on the selectin ligand activity afforded primarily by the activity of Fut7.

3.2) α(1,3)Fucosyltransferase-Dependent Alteration of Granulopoiesis.

The previous studies show that the expansion of IL-17-producing cells and the neutrophilia observed in $Fut^{-/-}$ mice are selectin dependent. We next sought to elucidate how selectin-ligand function can alter circulating neutrophil counts and IL-17 production. Based on the studies of Stark et al.[20], who proposed a trafficking-dependent regulatory feedback loop responsible for maintaining homeostatic granulopoiesis (Figure 1.2), we hypothesized that the IL-17-producing cell population expansion and neutrophilia were the result of the disruption of neutrophil trafficking leading to accelerated granulopoiesis.

3.2.1 In Vivo Manipulation of Granulopoiesis

Granulopoiesis is a tightly regulated process that requires constant feedback to monitor and maintain neutrophil numbers at steady state conditions, while keeping the system primed for rapid neutrophil production and release during infection or injury. $Fut^{-/-}$ mice have a leukocyte trafficking deficiency, a marked neutrophilia, and high plasma concentrations of IL-17 and G-CSF. Given these alterations in granulopoietic signaling, it was unclear whether $Fut^{-/-}$ animals would be capable of responding appropriately to regulatory stimuli for granulopoiesis. Therefore, WT and Fut-/- mice were injected with the

neutrophil specific Ly-6G (1A8) antibody to deplete circulating neutrophils. We hypothesized that the clearance of the circulating neutrophils would greatly increase efferocytosis–dependent IL-23 suppression, which would reduce IL-17 and G-CSF production, resulting in reduced neutrophil production. As shown in Figure 3.5A, following the injection of 1mg of 1A8, neutrophil counts in WT mice were quickly reduced by 90% and required 36 hours to fully recover. However, neutrophil counts remained unaltered in $Fut^{-/-}$ mice following antibody injection. To determine if that the lack of depletion was due to insufficient quantities of antibody, we injected 9mg of antibody into $Fut^{-/-}$ mice, with no effect on circulating neutrophil counts (Figure 3.5A). These results show that normal granulopoietic signals are disrupted in $Fut^{-/-}$ mice and suggest the clearance of antibody-labeled neutrophils may be a selectin-dependent process.

It remained unclear whether emergency granulopoiesis is intact in $Fut^{-/-}$ mice. To test this, we injected WT and $Fut^{-/-}$ mice with 1mg/kg LPS and monitored circulating neutrophil counts over 48 hours. After 12 hours, neutrophil counts were significantly increased in both WT and $Fut^{-/-}$ mice (Figure 3.5B). The increases in neutrophil counts peaked near 24 hours for both WT and $Fut^{-/-}$ mice at 50% and 80% of circulating leukocytes respectively. By 48 hours, neutrophil counts for WT and $Fut^{-/-}$ mice had returned to baseline. These results clearly show that

emergency granulopoiesis is still in tact in $Fut^{-/-}$ mice, indicating that the signaling mechanisms involved (TLR, NF-κB, etc.) may be distinct from those signaling mechanisms regulating homeostatic granulopoiesis.

3.2.2 α(1,3)Fucosylated Glycans on Myeloid Cells Regulate Granulopoiesis.

Because the enhanced granulopoiesis is associated with increased IL-17 production in $Fut^{-/-}$ mice, I sought to assess the contribution of myeloid cells to the enhanced IL-17 production and neutrophilia observed in $Fut^{-/-}$ mice. Two novel transgenic mouse lines were utilized: $Fut^{-/-}$c-FMS-FUT7-Tg (Tg-Fut) and $Fut4^{-/-}$c-FMS-CRE-Loxp-FUT7 (Cre-Fut). As shown in the schematic in Figure 3.6A, the Tg-Fut mouse is globally deficient in both FUT4 and FUT7, but carries FUT7 transgene driven by the myeloid-specific c-FMS promoter. The result is re-expression of Fut7 in myeloid cells, allowing them to traffic normally while all other cell populations retain a selectin-dependent trafficking deficiency (Table 3.4).

The Cre-Fut mouse was generated by crossing a $Fut4^{-/-}$ mouse that expressed a c-FMS driven Cre recombinase transgene, with a $Fut4^{-/-}$ mouse with a floxed FUT7 allele. The resulting mouse (Cre-Fut) has Cre expressed only in myeloid cells. Once expressed the Cre interacts with the Loxp sites to excise the FUT7 gene (Figure 3.6B). This creates Fut4/Fut7 deficient myeloid cells which are unable to utilize selectin-

dependent trafficking, while all other leukocyte populations retain Fut7 expression and can traffic normally (Table 3.4).

The genetic manipulations in the Cre-Fut and Tg-Fut mice allow us to determine if the neutrophilia and IL-17 alterations are dependent exclusively on myeloid cell trafficking. As shown in Figure 3.6C, Tg-Fut mice had normal circulating numbers of neutrophils, monocytes, and lymphocytes, while the Cre-Fut mice recapitulated the leukocytosis and neutrophilia found in $Fut^{-/-}$ mice. Flow cytometric analysis of splenic IL-17-producing cell populations show that Tg-Fut mice have WT numbers of Th17, NKT, γδ Tcells, and ILCs, while Cre-Fut mice had a 10-fold increase in Th17, a 19-fold increase in NKT, a 16-fold increase in ILC, and a 20-fold in γδ Tcell counts compared to WT and Tg-Fut mice (Figure 3.6D). These results show that myeloid cell trafficking is responsible for the Fut-dependent alterations in granulopoiesis.

3.2.3 Tcells Are Not Required for Fut-Dependent Alterations in Granulopoiesis

IL-17 is normally thought to be produced by Tcells (Th17, γδ, NKT), suggesting we could dampen the exaggerated granulopoietic signaling in $Fut^{-/-}$ mice by depleting the Tcell sources of IL-17. To test this hypothesis we crossed $Rag1^{-/-}$ mice, which lack functional B-cells and Tcells, with our $Fut^{-/-}$ mice to generate $Rag1^{-/-}/Fut^{-/-}$ mice. These mice were used to

assess the role of B-cells and Tcells in the Fut-dependent granulopoietic phenotype. CBCs were performed on whole blood isolated from WT, $Fut^{-/-}$, or $Rag1^{-/-}/Fut^{-/-}$ mice (Figure 3.7). $Rag1^{-/-}/Fut^{-/-}$ mice retain a 3.5-fold increase in circulating leukocytes, a10-fold increase in neutrophils, a 3-fold increase in monocytes, and have a 9-fold reduction in circulating lymphocytes compared to WT mice. Thus, the Fut-dependent alterations in granulopoiesis do not rely on B-cells or Tcells to induce the increased neutrophil counts observed in $Fut^{-/-}$ mice. These data suggest there is a nonlymphoid cell that is capable of producing the IL-17 required to maintain the neutrophilia in $Fut^{-/-}$ mice.

3.2.4 Bone Marrow-Derived Cells are Responsible for the Neutrophilia and IL-17 Expansion in $Fut^{-/-}$ Mice.

The results from the $Rag1^{-/-}/Fut^{-/-}$ mouse show that B-cells and Tcell are not required to generate the neutrophilia, and may not be required for the IL-17-producing cell expansion. However, a myeloid cell trafficking deficiency is required to maintain the phenotypes observed in $Fut^{-/-}$ mice. Myeloid cells can reside in peripheral tissues or be derived from the bone marrow. To determine which of these two myeloid populations are responsible for the IL-17 expansion and neutrophilia, we performed bone marrow transplants (BMTs).

We quickly discovered that $Fut^{-/-}$ mice are more resistant to radiation then WT mice. As shown in Figure 3.8A, after 9gy of radiation, 100% of WT mice died, while only 20% of $Fut^{-/-}$ mice succumbed. It is interesting to note the studies by Lubberts et al.[96] that show that IL-17 protected cells from irradiation. We performed two series of BMT experiments. The first experiment used WT mice irradiated with the standard dose of 9gy as recipients of $1x10^7$ cells from WT or $Fut^{-/-}$ BM (Figure 3.8A). The second set of experiments used $Fut^{-/-}$ mice that were irradiated with 12gy as recipients of $1x10^7$ cells from WT or $Fut^{-/-}$ BM. Six weeks following BMT, mice were sacrificed and a CBC and analysis of IL-17-producing cell types were performed. We observed no difference in engraphment of WT or $Fut^{-/-}$ BM into WT recipients (Figure 3.8B). The CBC showed that transfer of WT BM into a WT recipient did not alter leukocyte counts, however when $Fut^{-/-}$ BM was transferred into a WT mice, a leukocytosis comprised of a 11-fold increase in neutrophils, a 3.8-fold increase in monocytes, and a 1.3-fold increase in circulating lymphocytes was observed (Figure 3.8C). These results show that the neutrophilia in $Fut^{-/-}$ is at least partially dependent on bone marrow derived cells.

We also quantified the population sizes of IL-17-producing cells in WT mice that received WT and $Fut^{-/-}$ BM. As shown in figure 3.8D, WT mice that were reconstituted with WT BM had normal populations of IL-

17-producing cells. WT mice that received $Fut^{-/-}$ BM however, had a 7-fold increase in Th17 cells, a 16-fold increase in NKT cells, a 19-fold increase in γδ Tcells, and a 12-fold increase in ILCs. Taken together, the CBC and cell population size data show that the expansion of IL-17-producing cells and neutrophilia are dependent on bone marrow-derived cells. Together with our results from the Tg-Fut and Cre-Fut mice, these data suggest that bone marrow-derived myeloid cell trafficking is responsible for the regulation of neutrophil counts and IL-17 production in vivo.

To determine if bone marrow-derived cells were solely responsible for regulating neutrophil counts and IL-17 production, we transplanted WT and $Fut^{-/-}$ BM into $Fut^{-/-}$ mice that had been lethally irradiated with 12gy ionizing radiation. Transfer of $Fut^{-/-}$ BM into $Fut^{-/-}$ mice had no effect on leukocyte counts or population size of IL-17-producing cells (Figure 3.9B/C). When WT BM was transferred into $Fut^{-/-}$ mice, circulating leukocyte counts dropped to near WT levels. This was manifest by a 75% reduction in circulating leukocytes, an 80% reduction in neutrophil counts, a 70% reduction in monocytes, and a 20% reduction in lymphocyte counts compared with $Fut^{-/-}$ mice that received $Fut^{-/-}$ BM (Figure 3.9B). The IL-17-producing cell populations were also reduced in $Fut^{-/-}$ mice that received WT BM. We observed an 80% reduction in Th17 cells, an 88% reduction in NKT cells, a 90% reduction in γδ Tcells, and an

85% reduction in ILCs compared to $Fut^{-/-}$ mice with $Fut^{-/-}$ BM (Figure 3.9C).

The results from the BMT studies show that bone marrow-derived cell trafficking is responsible for the expansions of IL-17-producing cells and the neutrophilia observed in $Fut^{-/-}$ mice. Together, these results significantly reduce the number of cell types that may be involved in the regulation of granulopoiesis to macrophages, dendritic cells, and immature neutrophils. However, additional studies are required to identify which specific cell type is responsible for the IL-17-producing cell expansion and neutrophilia observed in $Fut^{-/-}$ mice.

3.2.5 Neutrophil Trafficking to Tissue Resident Macrophages Regulates Granulopoiesis

Our previous experiments (Figures 3.8 & 3.9) determined that Fut-dependent trafficking of bone marrow derived myeloid cells is responsible for the regulation of granulopoiesis, so I next sought to identify the specific cell type responsible. I hypothesized that loss of Fut-dependent neutrophil trafficking was responsible for the dysregulation of granulopoiesis. To test this hypothesis I developed an adoptive neutrophil transfer protocol. Neutrophils were isolated from BM of WT and $Fut^{-/-}$ mice, labeled with a cell tracker dye (CMPTX-Red or CMFDA-Green), and injected i.v. into $Fut^{-/-}$ mice (Figure 3.10A). Mice were

sacrificed 24 hours post injection and circulating neutrophil counts and neutrophil tissue infiltration was assessed via flow cytometry.

As shown in Figure 3.10B, transfer of $Fut^{-/-}$ neutrophils into $Fut^{-/-}$ mice, did not alter circulating neutrophil counts. Transfer of WT neutrophils into $Fut^{-/-}$ mice however, reduced circulating neutrophil counts by 50%. Additionally, mononuclear leukocytes were isolated from the liver and spleen and analyzed for CFMDA. A cell that was Ly-$6G^{-}$ $CMFDA^{+}$ was determined to be a phagocyte that had ingested a transferred neutrophil. We found that an equal percentage (23%) of WT and $Fut^{-/-}$ labeled neutrophils were phagocytosed in the spleen of $Fut^{-/-}$ mice (Figure 3.10C). Interestingly, we found that nearly 8 times as many WT neutrophils were cleared by the liver then $Fut^{-/-}$ neutrophils. These findings suggest differential neutrophil trafficking requirements between the spleen and liver, and suggest that neutrophil trafficking to the spleen is not Fut-dependent. These results also suggest that neutrophil trafficking to the liver is at least partially Fut-dependent, and is responsible for regulating homeostatic granulopoiesis.

3.2.6 $Fut^{-/-}$ Phagocytes Have No Defect in Phagocytic Rate, IL-23 Expression, or IL-23 Production.

The results from our previous experiments suggested that neutrophil trafficking is required for the maintenance of normal circulating

neutrophil counts. It is possible that loss of Fut4/7 alters tissue resident phagocyte function. Therefore, we assessed the phagocytic function, IL-23 expression, and IL-23 production in tissue resident or BM-derived phagocytes isolated from WT and $Fut^{-/-}$ mice. The proposed granulopoiesis-related functions of bone marrow-derived macrophages (BM-MCs) and primary Kupffer cells (pKCs) isolated from WT and $Fut^{-/-}$ mice were assessed in vitro. BM from WT and $Fut^{-/-}$ mice was cultured for 7 days with M-CSF to differentiate the BM cells into $CD11b^{+}$ bone marrow-derived macrophages (BM-MC). As shown in figure 3.11A, no difference was observed between WT and $Fut^{-/-}$ marrow in the ability to differentiate BM cells to BM-MCs. After confirming that BM-MCs were $CD11b^{+}$ via flow cytometry, BM-MCs were incubated with CMFDA labeled neutrophils isolated from WT mice. After four hours BM-MCs were assessed via flow cytometry for CMFDA as a measure of phagocytic rate. No difference in phagocytic rate was observed between WT and $Fut^{-/-}$ BM-MCs, as approximately 70% of $CD11b^{+}$ BM-MCs from each genotype had ingested at least one labeled neutrophil (Figure 3.11B).

Granulopoietic regulation is thought to rely heavily on phagocyte IL-23 production, so IL-23 gene expression and protein production was assessed in BM-MCs following LPS stimulation. As shown in Figure 3.11C, there was no difference in IL-23 gene expression or protein production

between WT and Fut$^{-/-}$ BM-MCs. These results demonstrate that there is no overt defect in these granulopoiesis-related functions of Fut$^{-/-}$ BM-MCs.

Because the results of the adoptive neutrophil transfer experiments suggested that the liver was a major site of neutrophil clearance, we isolated pKCs from WT and Fut$^{-/-}$ mice and compared their function. After perfusion and enzymatic digestion of the liver, pKCs were isolated by centrifugation, and purity was assessed via F4/80 positivity by flow cytometry. As shown in Figure 3.11D, there was no difference in the number of pKCs isolated from WT or Fut$^{-/-}$ livers. pKCs were then incubated with labeled WT neutrophils and phagocytic rate was determined via flow cytometry. No difference was observed in the phagocytic rate of pKCs from WT or Fut$^{-/-}$ livers (Figure 3.11E). Lastly, LPS stimulated pKCs were harvested and IL-23 gene expression and protein levels were quantified via qPCR and ELISA. Figure 11F shows that there is no difference between IL-23 expression or protein levels between WT and Fut$^{-/-}$ mice. These results suggest that Fut$^{-/-}$ BM-MC and pKCs are not deficient in their ability to phagocytose neutrophils, induce IL-23 expression, or secrete IL-23 protein.

3.2.7 Efferocytosis Does Not Suppress IL-23 Expression or Production

IL-23 produced by phagocytes in peripheral tissues is thought to maintain granulopoietic signaling. Phagocyte clearance of apoptotic

neutrophils, called efferocytosis, is thought to suppress IL-23 production in phagocytes, dampen granulopoietic signaling, and reduce the number of neutrophils being released from the bone marrow. I hypothesized that efferocytosis-dependent IL-23 suppression was reduced in $Fut^{-/-}$ mice due to the neutrophil trafficking deficiency, contributing to the increased granulopoietic signaling and neutrophilia. An in vitro efferocytosis assay was used to assess the effect of efferocytosis on phagocytes isolated from WT or $Fut^{-/-}$ mice.

Phagocytes isolated from WT and $Fut^{-/-}$ mice were stimulated with LPS to induce IL-23 expression and protein production, then WT apoptotic neutrophils were incubated with the phagocytes for four hours. Messenger RNA and cell culture supernatants were collected, and IL-23 was assessed via qPCR and ELISA. As shown in Figure 3.12A, WT and $Fut^{-/-}$ phagocytes induced IL-23 gene expression at equal levels for pKCs, BM-MCs, and Bone Marrow Derived Dendritic Cells (BM-DCs). However, after incubation with apoptotic neutrophils, we were unable to detect an alteration in IL-23 gene expression. Similarly, when IL-23 production was assessed via ELISA, no difference among WT and $Fut^{-/-}$ pKCs, BM-MCs, or BM-DCs was observed (Figure 3.12B). Incubation with apoptotic neutrophils had no effect on IL-23 production by WT or $Fut^{-/-}$ pKCs, BM-MCs, and BM-DCs.

These results were unexpected. There was no difference between WT and $Fut^{-/-}$ efferocytosis, and there was also no detectable alteration in IL-23 at the transcript or protein level. This suggests that either the proposed regulatory model of granulopoiesis is incomplete and that an additional factor is required to modulate IL-23, or that BM-MCs, BM-DC, and pKCs are not involved in maintaining normal granulopoiesis. Considering all of the data together, I hypothesize that the model is incomplete and that there are additional factors, yet to be discovered that contribute to the regulation of granulopoiesis.

3.3) Loss of α(1,3)Fucosylated Glycans Increases the Severity of DSS-Induced Colitis

Dextran Sodium Sulfate (DSS)-induced colitis is a common model of mucosal injury used to model human ulcerative colitis, and in some cases Crohn's disease. The disease pathogenesis relies heavily on IL-23, IL-17, and leukocyte trafficking. Because of the contrasting phenotypes found in $Fut^{-/-}$ mice (proinflammatory elevations in IL-17 and anti-inflammatory trafficking defect) we wanted to establish whether the loss of α(1,3) fucosylation altered the initiation of mucosal injury during DSS colitis. We hypothesized that the enhanced IL-17 production, coupled with the pronounced increase in $\gamma\delta$ Tcells in $Fut^{-/-}$ mice will cause a more rapid and severe colitis than in WT mice.

To induce disease, 3% DSS was added to the drinking water of WT or $Fut^{-/-}$ mice for 5 days, followed by 0, 3, or 5 days of untreated water as a recovery period. Weight and occult rectal bleeding were monitored daily. At the completion of the experiment colons were removed, fixed, sectioned, stained with Hematoxylin and Eosin, and scored for disease severity.

3.3.1 Ten Day Time Point

At the 10 day time point (5 days DSS + 5 days water; as shown in figure 3.13A), all WT mice survived and all of the $Fut^{-/-}$ mice died. Over the course of the experiment (Figure 3.13B), $Fut^{-/-}$ mice lost more weight, more rapidly, then WT mice. Unfortunately the demise of the $Fut^{-/-}$ mice did not allow us to histologically assess disease severity.

3.3.2 Eight Day Time Point

The protocol was shortened to an 8 day experiment (5 days DSS + 3 days water). At this time point all the WT and 80% of $Fut^{-/-}$ mice survived to the end of the experiment (Figure 3.14A). By the end of the experiment $Fut^{-/-}$ mice lost 10% more weight then WT mice (Figure 3.14B). However, when histologic scores were tabulated and compared, there was severe disease in both groups with no significant difference between WT and $Fut^{-/-}$ mice (Figure 3.14C). These results were

surprising, as the physical signs of disease had suggested that the $Fut^{-/-}$ mice were experiencing more severe disease. The severe histology suggests that an even shorter experiment may be necessary to differentiate between groups.

Tcells are not thought to play a significant role in the development of colitis, however γδ Tcells are the major source of intestinal IL-17 that is important for the pathogenesis of colitis. Therefore the $Rag1^{-/-}$ and $Rag1^{-/-}/Fut^{-/-}$ mice were tested to determine if Tcell trafficking contributes to the disease severity observed in $Fut^{-/-}$ mice. $Rag1^{-/-}$ mice had very severe colitis, and 50% of $Rag^{-/-}$ mice died before the final time point (Figure 3.14A) while none of the $Rag/Fut^{-/-}$ mice died. Both $Rag1^{-/-}$ and $Rag1^{-/-}/Fut^{-/-}$ mice lost more weight then WT and $Fut^{-/-}$ mice by the end of the experiment (Figure 3.14B). Interestingly, $Rag1^{-/-}$ mice did have significantly more severe disease then WT and $Fut^{-/-}$ mice, however the $Rag1^{-/-}/Fut^{-/-}$ mice did not have increased disease severity compared to WT and $Fut^{-/-}$ (Figure 3.14C).

These results suggest that $Fut^{-/-}$ mice have more severe symptoms of disease (decreased survival, increased weight loss, increased occult rectal bleeding) then WT mice, which was not supported by the histology at 8 days. This could be explained by a possible difference in the rate of disease progression. In addition, the strong increase in disease severity of the $Rag1^{-/-}$ mice shows that Tcells and/or Bcells play a protective role

in the pathogenesis of colitis. The loss of this protection in the $Rag1^{-/-}$ mice allows for addition inflammation and mucosal damage. Loss of Fut-dependent trafficking in the $Rag1^{-/-}/Fut^{-/-}$ mice reduces disease severity, suggesting that Fut-dependent recruitment of a non-lymphoid population of leukocytes significantly contributes to disease severity.

3.3.3 Five Day Time Point

The protocol was shortened to a 5 day experiment (5 days DSS treatment). At this time point all mice survived to the end of the experiment. $Fut^{-/-}$ mice lost 5% more weight then WT mice over the course of the experiment (Figure 3.15A). Histologic scoring of the colitis showed that $Fut^{-/-}$ mice had histology score of 17 compared to a score of 8 in WT mice, indicating that $Fut^{-/-}$ mice have a significantly more severe colitis then WT mice (Figure 3.15B). These data show that loss of α(1,3)-fucosylation on leukocytes exacerbates mucosal injury in DSS-colitis.

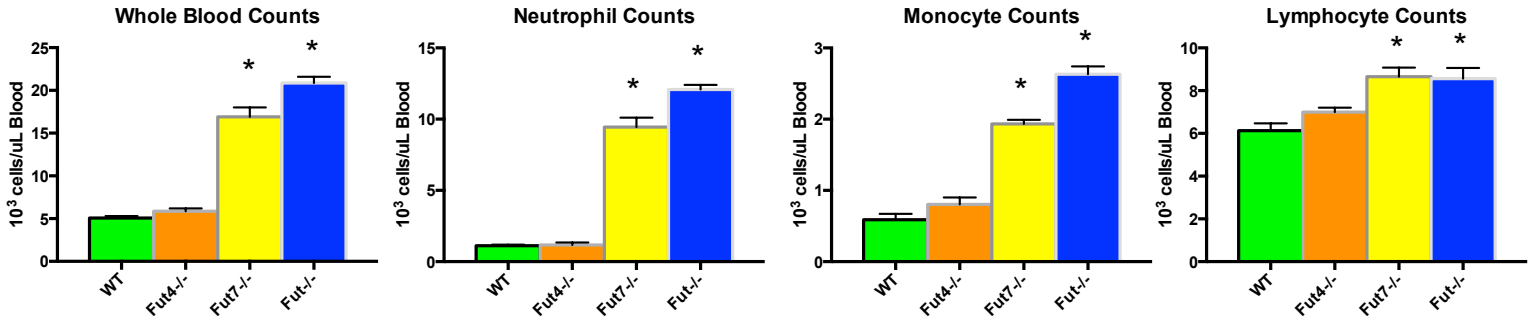

Figure 3.1. Leukocyte counts in Fut$^{-/-}$ Mice
Whole blood was drawn from WT, Fut4-/-, Fut7-/-, Fut-/- mice and circulating leukocyte counts were assessed with an automated blood counter. Data presented as mean ± standard error. n=6 mice / genotype. *=$p<0.05$

	WT	Fut$^{-/-}$	WT LPS	Fut$^{-/-}$ LPS
IL-1α	56.2 ± 1.6	57.7 ± 6.6	50.0 ± 2.1	58.2 ± 1.5 ₸
IL-1β	465.1 ± 52.4	635.7 ± 87.2	657.7 ± 46.2	827.5 ± 46.2 ₸
IL-2	153.5 ± 14.8	182.0 ± 26.2	125.0 ± 4.1	128.0 ± 9.0
IL-3	21.8 ± 2.8	24.8 ± 2.4	24.6 ± 4.4	19.9 ± 1.9
IL-4	18.8 ± 5.6	27.8 ± 3.8	25.1 ± 3.3	27.7 ± 2.0
IL-5	55.0 ± 8.4	78.3 ± 11.0	91.6 ± 16.6	77.2 ± 23.6
IL-6	16.2 ± 1.6	22.8 ± 4.2	186.1 ± 52.6	753.5 ± 162.8 ₸
IL-10	168.0 ± 12.8	194.1 ± 27.0	523.1 ± 47.7	929.0 ± 27.0 ₸
IL-12(p40)	369.8 ± 14.9	321.1 ± 35.5	853.0 ± 203.9	923.9 ± 80.0
IL-12(p70)	248.9 ± 20.5	311.5 ± 22.7	297.0 ± 42.5	381.6 ± 43.6
IL-13	653.8 ± 117.2	1054.8 ± 94.6 *	376.9 ± 103.3	491.4 ± 24.1
IL-17	83.5 ± 16.8	211.1 ± 26.0 *	95.3 ± 10.3	270.5 ± 41.1 ₸
Eotaxin	2400.4 ± 211.3	2440.4 ± 143.6	3464.7 ± 120.1	2768.1 ± 121.5 ₸
G-CSF	93.0 ± 7.8	511.4 ± 55.5 *	14356.8 ± 6227.2	29795 ± 2297.0 ₸
GM-CSF	341.6 ± 10.8	366.5 ± 30.1	599.0 ± 22.6	549.8 ± 34.7
IFNγ	44.3 ± 3.4	48.5 ± 4.0	55.0 ± 3.7	50.0 ± 2.9
KC	85.0 ± 9.4	90.6 ± 12.6	425.1 ± 97.0	490.0 ± 113.1
MCP-1	658.2 ± 76.3	896.0 ± 55.3 *	1551.4 ± 207.0	1096.1 ± 28.3 ₸
MIP-1α	49.8 ± 2.8	65.1 ± 4.4 *	109.9 ± 5.3	136.9 ± 11.8 ₸
MIP-1β	206.6 ± 26.7	251.6 ± 18.8	326.4 ± 20.0	235.9 ± 15.8 ₸
RANTES	81.9 ± 3.0	76.6 ± 13.2	1402.4 ± 300.4	2217.0 ± 220.9
TNFα	2106.2 ± 303.9	2695.1 ± 187.3	3244.7 ± 114.2	2684.1 ± 161.6 ₸

Table 3.1 – Alterations in Circulating Cytokine Levels
Whole blood was drawn from untreated or LPS stimulated (1mg/kg) WT and Fut-/- and plasma was isolated. A bio-plex cytokine assay was performed. All results are in pg/mL and present as mean ± standard error. n=5-7 mice / condition / genotype. *=p≤0.05 vs WT unstimulated. ₸=p≤0.05 vs WT LPS

Cytokine	Fold Change vs. WT	
IL-13	1.6	p=.01
IL-17	2.5	p=.001
G-CSF	5.5	p<.0001
MCP-1	1.4	p=.02
MIP-1α	1.3	p=.01

Table 3.2 - Cytokine alterations in unstimulated Fut$^{-/-}$ Mice
Data presented as fold change over WT unstimulated mice
Data from Table 3.1

Cytokine	Fold Change vs. WT+LPS	
IL-1α	1.2	p=.01
IL-1β	1.25	p=.03
IL-6	4.1	p=.01
IL-10	1.8	p=.007
IL-17	2.9	p=.003
Eotaxin	-1.25	p=.003
G-CSF	2.1	p=.02
MCP-1	-1.4	p=.05
MIP-1β	-1.4	p=.007
TNFα	-1.2	p=.02

Table 3.3 - Cytokine alterations in LPS Stimulated Fut$^{-/-}$ Mice
Data presented as fold change over WT LPS stimulated mice
Data from Table 3.1

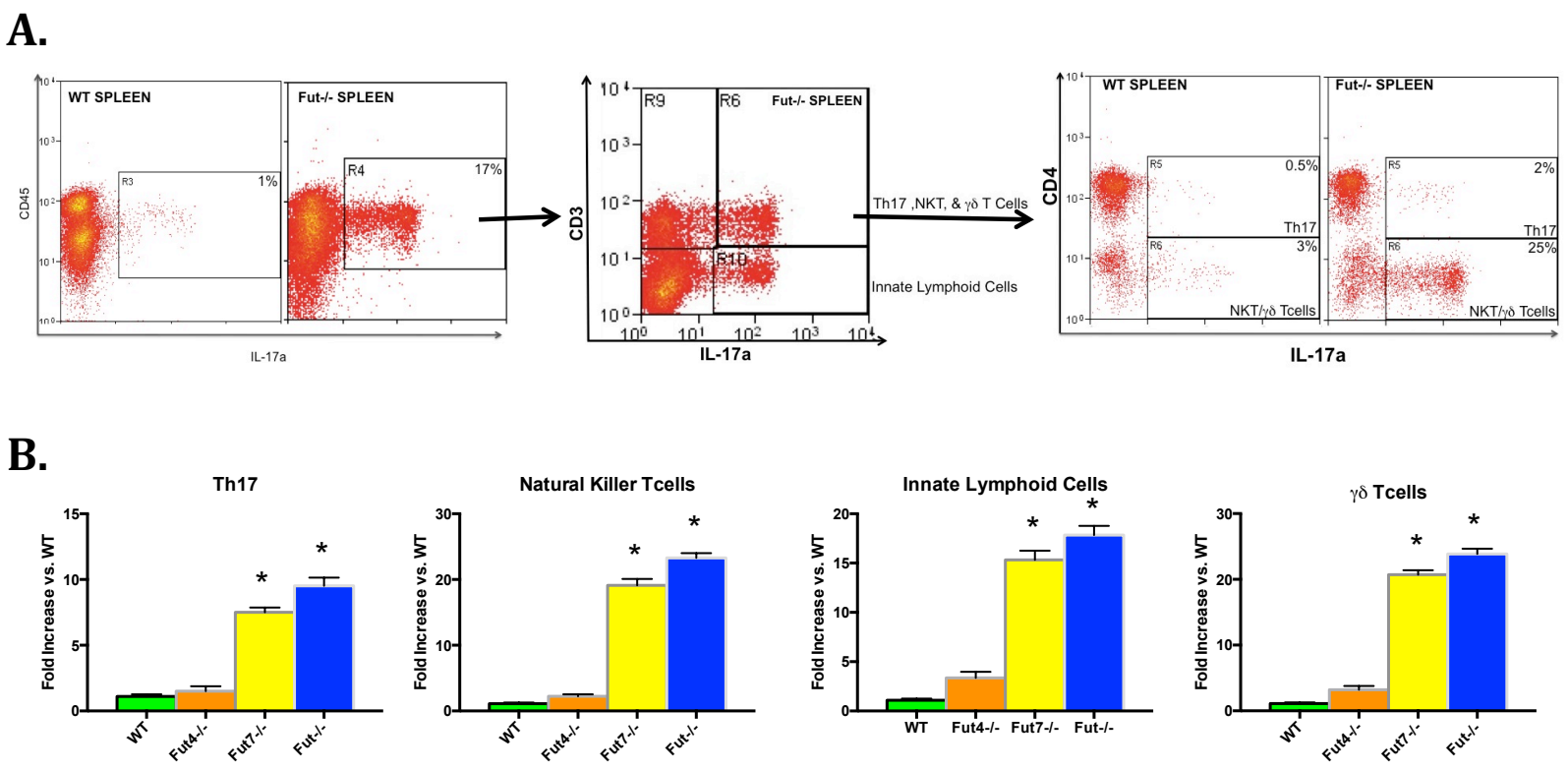

Figure 3.2. Enhanced IL-17 Production in Fut$^{-/-}$ mice.

A. Representative histogram of flow cytometric assessment of IL-17 production from mononuclear splenocytes from WT and Fut$^{-/-}$ mice stimulated with PMA/ION. CD45^{+} are selected and broken down by CD3 staining and CD4 staining. Fut$^{-/-}$ mice have more IL-17 producing Th17, NKT, γδ Tcells and ILCs then WT mice. Images representative of 4 individual experiments, n=3 mice per experiment. **B.** Quantification of IL-17-producing cell populations by flow cytometry. Th17 (CD3^{+}CD4^{+}IL-17^{+}), NKT (CD3^{+}DX5^{+}CD1d^{+}IL-17^{+}), γδ Tcells (CD3^{+}CD4^{-}γδTCR^{+}IL-17^{+}), and ILC (CD3^{-}CD4^{-}CD8^{-}NK1.1^{-}B220^{-}γδTCR^{-}CD45^{+}IL-17^{+}) were quantified from WT, Fut4$^{-/-}$, Fut7$^{-/-}$ and Fut$^{-/-}$ mice. Fut4-/- mice have WT numbers of IL-17 producing cells, while Fut7 have elevated levels of Th17, NKT, γδ Tcells and ILC indicating that Fut7 is primarily responsible for enhanced IL-17 production. n= 12 mice/genotype. *=p≤0.05

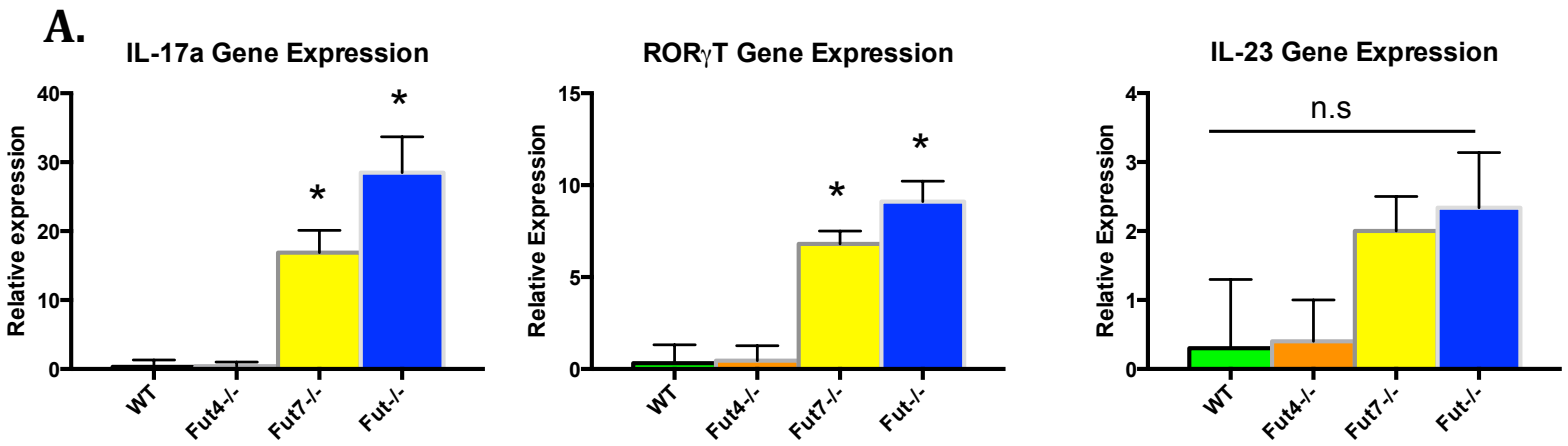

Figure 3.3- Enhanced IL-17 Production Is Not Due To Altered Tcell Differentiation

A. mRNA was isolated form PMA/ION stimulated mononuclear splenocytes, converted to cDNA and gene expression was assessed via qPCR. Gene expression levels of RORγt, IL-17 and IL-23 were standardized to βactin. Fut$^{-/-}$ mice have elevated gene expression levels of IL-17 and RORγt compared to WT and Fut4$^{-/-}$ mice. Data presented as mean ± standard error. n=6 mice / genotype. *=p≤.05

B. Naïve CD4 Tcells were harvested from WT of Fut$^{-/-}$ mice and incubated with TGFβ, IL-6, and IL-23 to differentiate the Tcells into Th17 cells. No difference was observed in Th17 differentiation between WT and Fut$^{-/-}$ Tcells. n= 5 mice/genotype

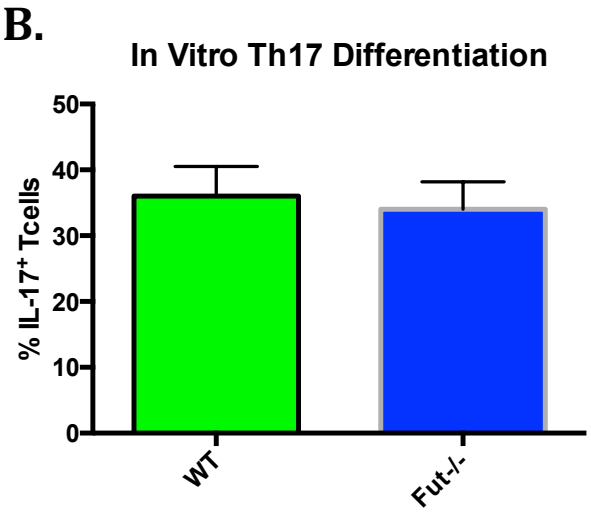

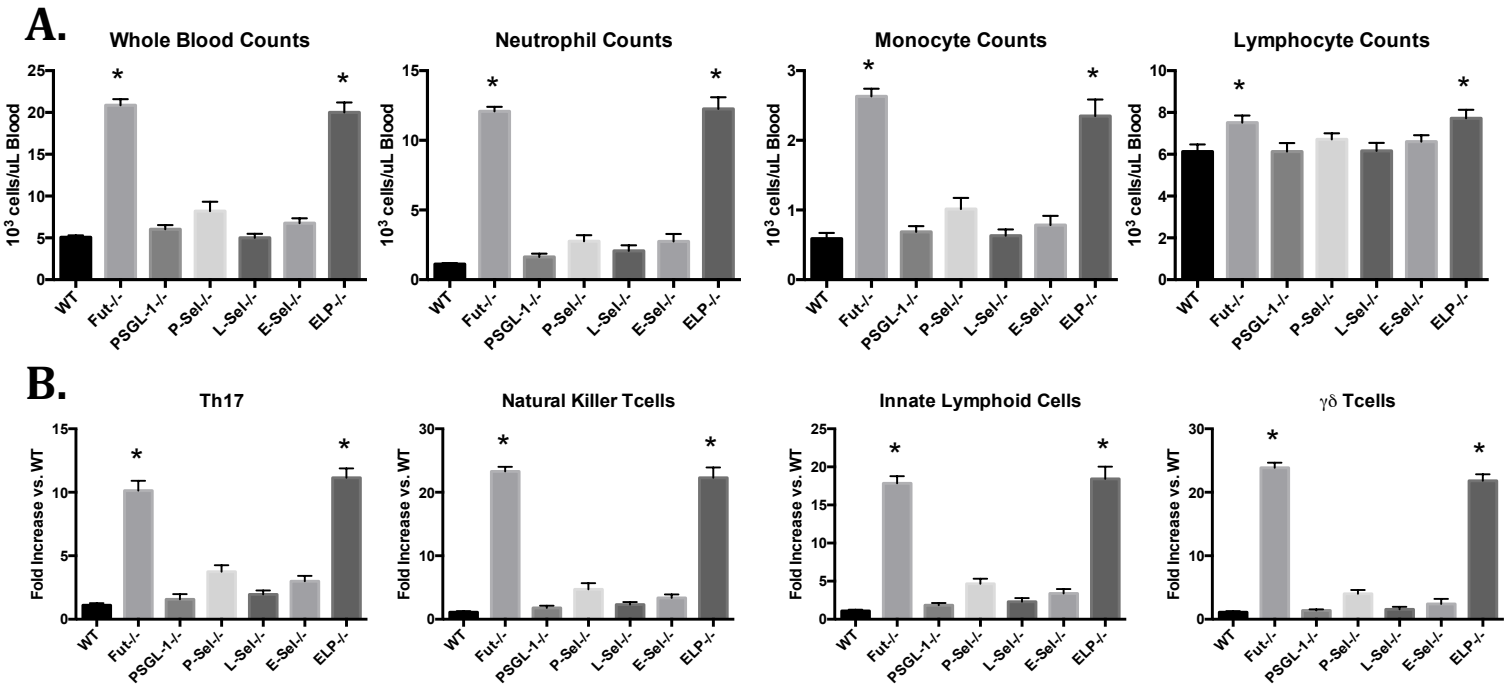

Fig 3.4 Fut-Dependent Neutrophilia and IL-17 production are Selectin-Dependent

A. A CBC was performed on whole blood from WT, Fut$^{-/-}$ PSGL-1$^{-/-}$, P-Sel$^{-/-}$, E-Sel$^{-/-}$, L-Sel$^{-/-}$, and ELP$^{-/-}$ mice. Individual selectin knockouts have WT leukocyte counts. However loss of all three selectins (ELP$^{-/-}$) recapitulates the leukocytosis observed in Fut$^{-/-}$ mice. Data presented as mean ± standard error. n=5 mice/genotype *=p≤0.05 **B.** IL-17-producing cell populations were assessed from mononuclear splenocytes from WT, Fut$^{-/-}$ PSGL-1$^{-/-}$, P-Sel$^{-/-}$, E-Sel$^{-/-}$, L-Sel$^{-/-}$, and ELP$^{-/-}$ mice via flow cytometry. ELP$^{-/-}$ mice have elevated number of Th17, NKT, ILC, γδ Tcells compared to WT and individual selectin deficient mice. Data presented as mean ± standard error. n=5 mice/genotype *=p≤0.05

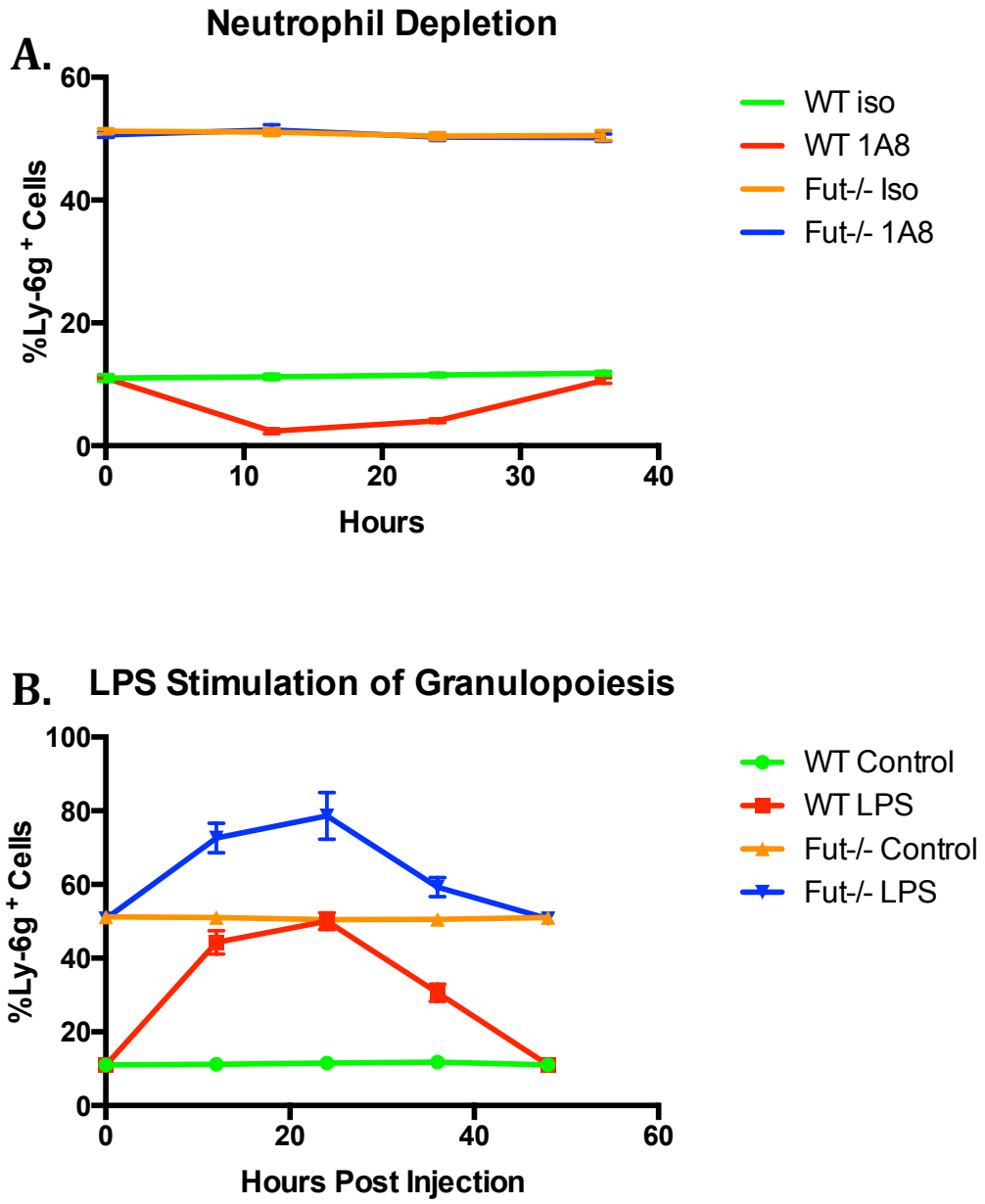

Figure 3.5. In Vivo Manipulation of Granulopoiesis
A. WT and Fut-/- mice were treated with 1mg and 9mg i.p. of 1A8 antibody and circulating neutrophil counts were monitored for 36 hours. WT neutrophils were quickly depleted from the blood stream, and took 36 hours to regain normal circulating levels. Fut-/- neutrophil counts remained unchanged for the duration of the experiment. n= 6 mice. **B.** WT and Fut-/- mice were injected i.p. with 1mg/kg LPS and circulating neutrophil counts were monitored for 48 hours. Both WT and Fut-/- circulating neutrophil counts increased for approximately 24 hours, then declined back to baseline by 48 hours. This indicates that Emergency Granulopoiesis is still inducible in Fut-/- mice. n=8 mice

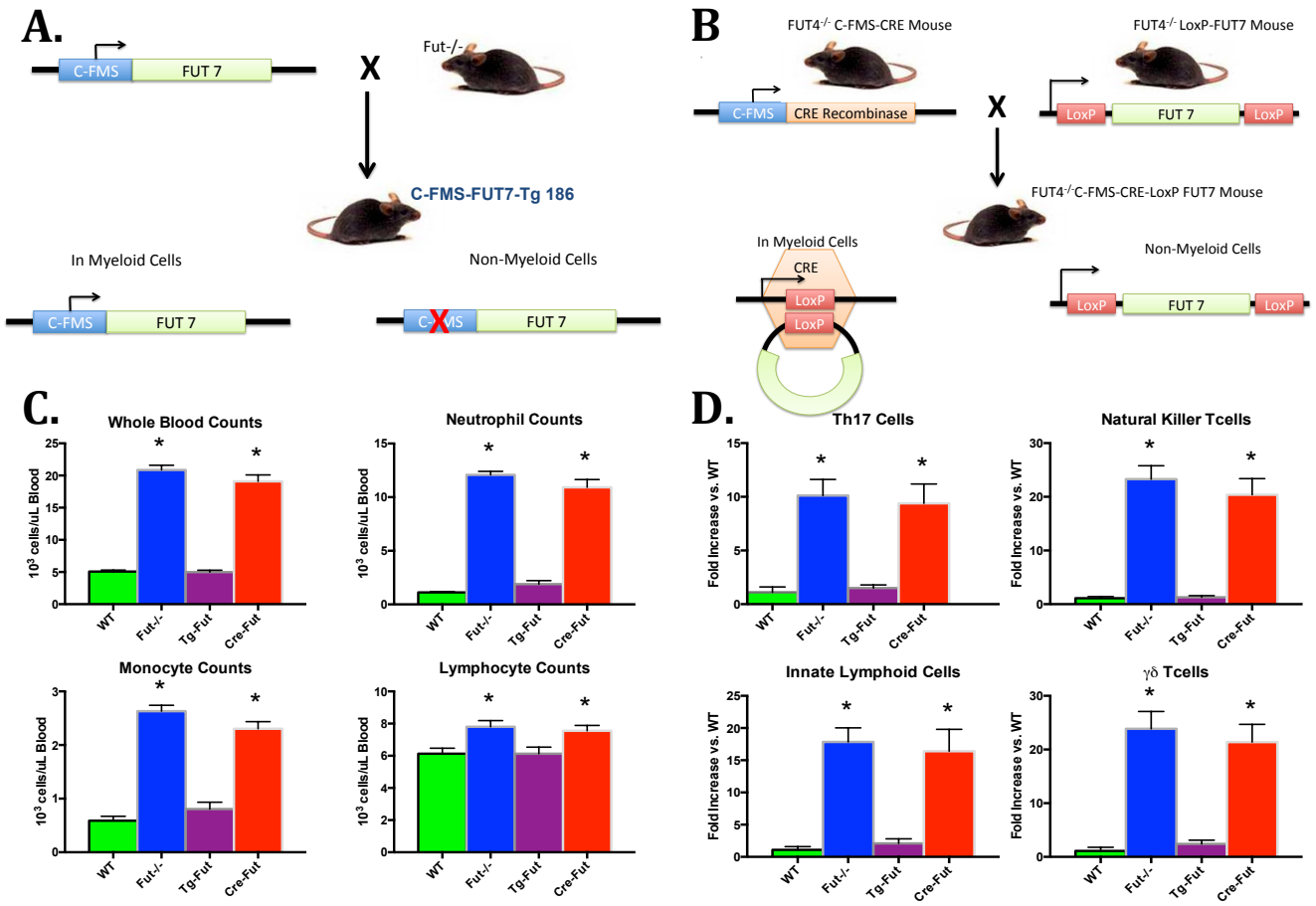

Figure 3.6. Myeloid Cell Trafficking is Required for Maintenance of Granulopoiesis and IL-17 Production.
A. Schematic detailing the generation of the Tg-Fut mouse. **B.** Schematic detailing the generation of the Cre-Fut mouse.
C. CBC of blood from WT, Fut$^{-/-}$, Tg-Fut, and Cre-Fut show that Tg-Fut mice have WT numbers of circulating leukocytes, while Cre-Fut mice reconstitute the neutrophilia of Fut$^{-/-}$ mice. n=7 mice/genotype. **D.** Assessment of IL-17-producing cell population size in WT, Fut$^{-/-}$, Tg-Fut, and Cre-Fut mice show that Cre-Fut mice have Fut$^{-/-}$ numbers of Th17, NKT, ILC, and γδTcells, while Tg-Fut mice have WT numbers of IL-17 producing cells. n=7 mice/genotype. Data presented as mean ± standard error. n=5 mice/genotype *=p≤0.05

Genotype	Cell Type	FUT 4	FUT 7	Trafficking Phenotype
WT	Myeloid	+	+	Normal
	Non-Myeloid	+	+	
$Fut^{-/-}$	Myeloid	-	-	Global Deficiency
	Non-Myeloid	-	-	
Tg-Fut	Myeloid	-	+	Normal Myeloid
	Non-Myeloid	-	-	
Cre-Fut	Myeloid	-	-	Deficient Myeloid
	Non-Myeloid	-	+	

Table 3.4. Summary of Leukocyte Trafficking abilities.

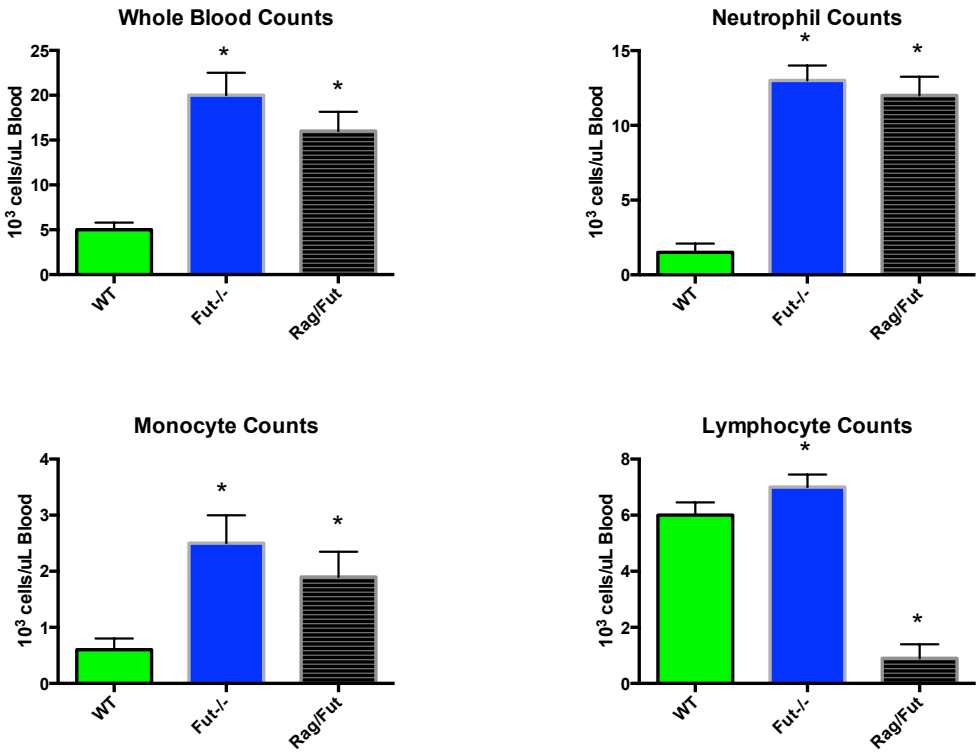

Figure 3.7. Lymphoid Cells Not Required For Fut-Dependent Neutrophilia

CBC was performed on blood from Rag1$^{-/-}$/Fut$^{-/-}$, WT, and Fut$^{-/-}$ mice. Rag1$^{-/-}$/Fut$^{-/-}$ have a leukocytosis with a 10-fold increase in circulating neutrophil counts compared to WT mice. n=4 mice/genotype. Data presented as mean ± standard error. *=p≤0.05

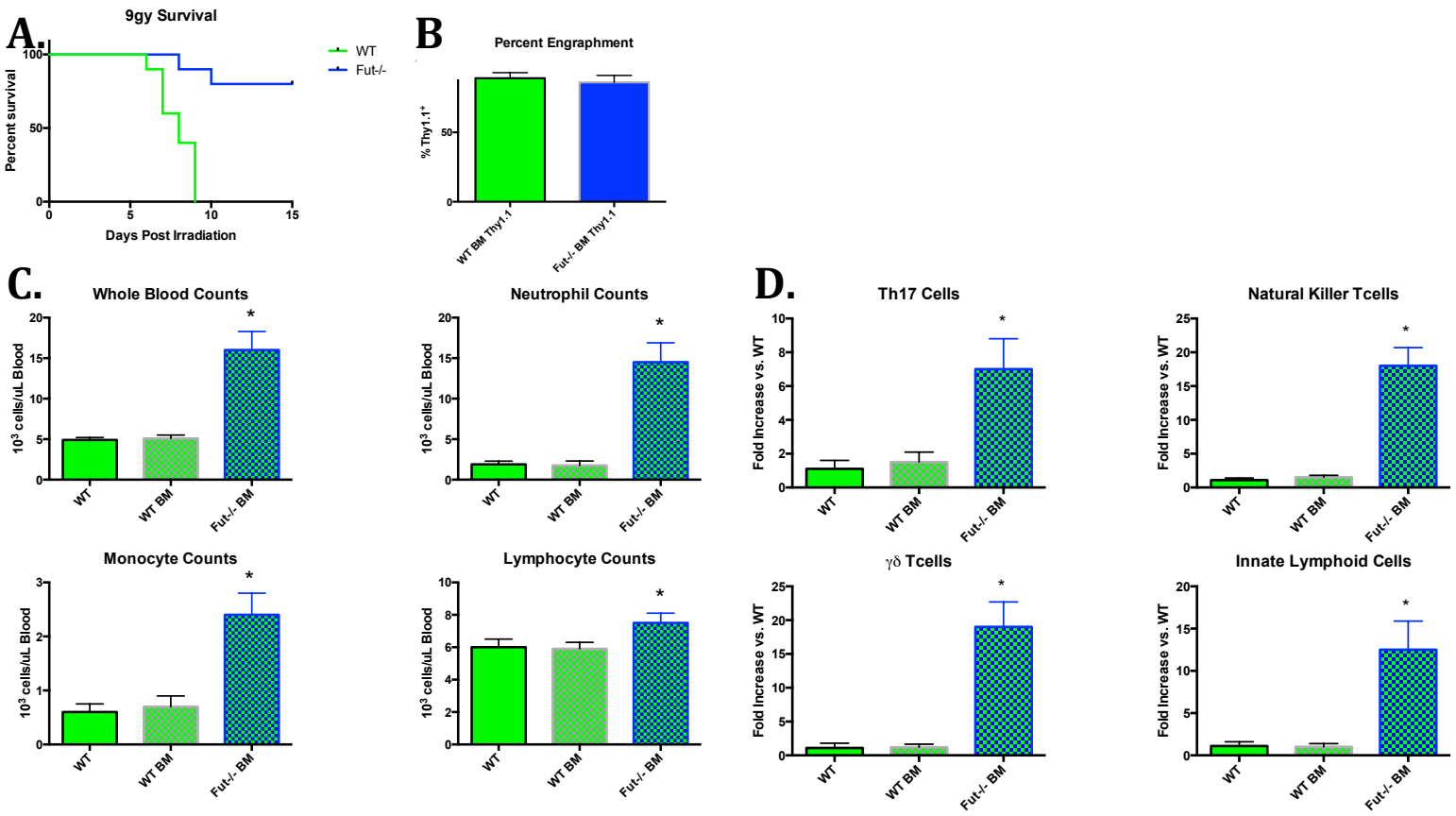

Figure 3.8. Transfer of Fut$^{-/-}$ BM into Lethally Irradiated WT Mice Reconstitutes the Neutrophilia and IL-17-producing cell expansions in Fut$^{-/-}$ mice

A. Survival of WT and Fut$^{-/-}$ mice irradiated with 9gy. 80% Fut$^{-/-}$ mice survived while all WT mice succumbed. n=10 mice/genotype. Following 9gy lethal irradiation, WT (thy1.1) mice received 1x10^{7} WT (thy1.2) or Fut$^{-/-}$ (thy1.2) BM cells i.v. 6 weeks post transplantation mice were sacrificed and percent engraphment was determined by flow cytometric analysis of thy1.1 (host-derived) vs thy1.2 (donor-derived). **B.** There was no difference between the percent engraphment of WT or Fut$^{-/-}$ BM into WT thy1.1 mice. **C.** CBCs were performed no blood from chimeric mice. WT mice reconstituted with WT marrow had no change in circulating leukocyte counts. WT mice reconstituted with Fut$^{-/-}$ BM had a leukocytosis comprised of a marked neutrophilia. **D.** Mononuclear splenocytes from chimeric mice were assessed for IL-17 producing cells. WT mice reconstituted with WT BM had normal levels of Th17, NKT, ILC, and γδ Tcells, however WT mice that received Fut$^{-/-}$ BM had significantly more Th17, NKT, ILC, and γδ Tcells. These results show that BM-derived cells are at least partially responsible for the neutrophilia and IL-17-producing cell population expansion seen in Fut$^{-/-}$ mice. n=9 mice/condition. Data presented as mean ± standard error. *=p≤0.05

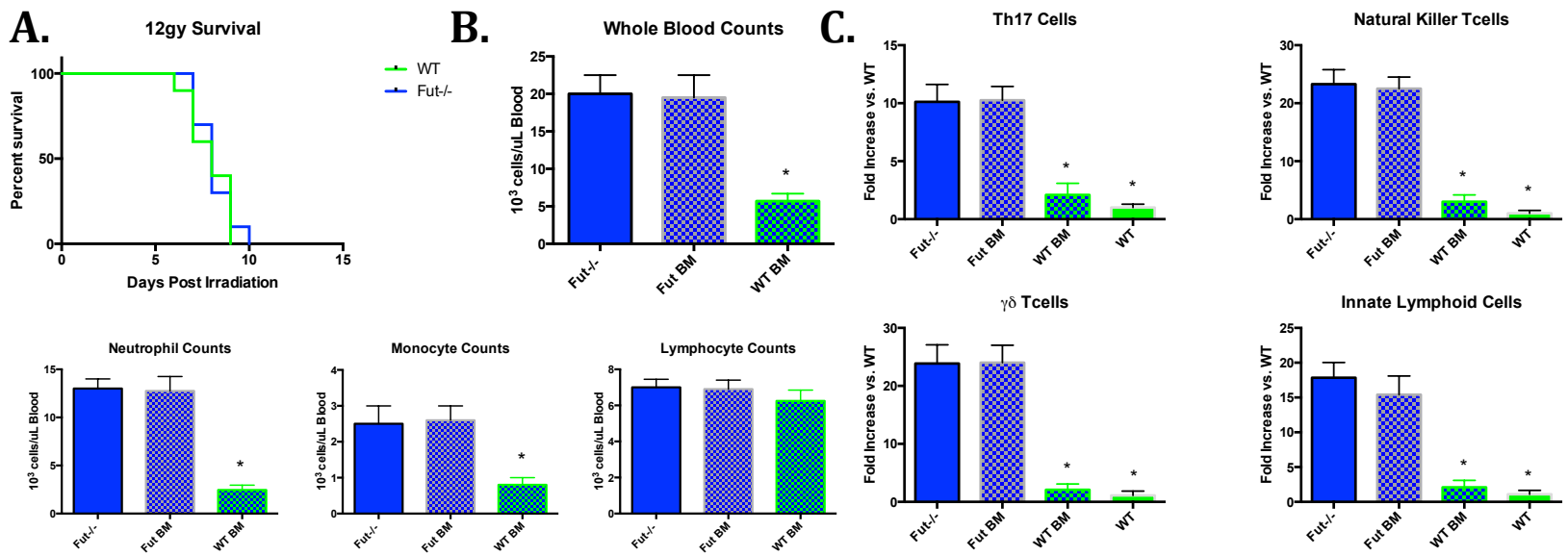

Figure 3.9 – Transplantation of WT BM in to a Lethally Irradiated Fut$^{-/-}$ Restores WT Neutrophil and IL-17-Producing Cell Counts.

A. Following irradiation with 12gy, WT and Fut$^{-/-}$ mice succumbed at the same rate. **B.** CBC was performed on blood from chimeric mice. Fut$^{-/-}$ mice that received Fut$^{-/-}$ BM had a leukocytosis, Fut$^{-/-}$ mice reconstituted with WT BM had WT leukocyte counts. **C.** IL-17-producing populations were assessed in Fut$^{-/-}$ mice that received WT BM had WT numbers of Th17, NKT, γδ Tcells, and ILCs while Fut$^{-/-}$ mice that received Fut$^{-/-}$ BM had elevated numbers of IL-17-producing cells. n=12 mice/condition. Data presented as mean ± standard error. *=p≤0.05

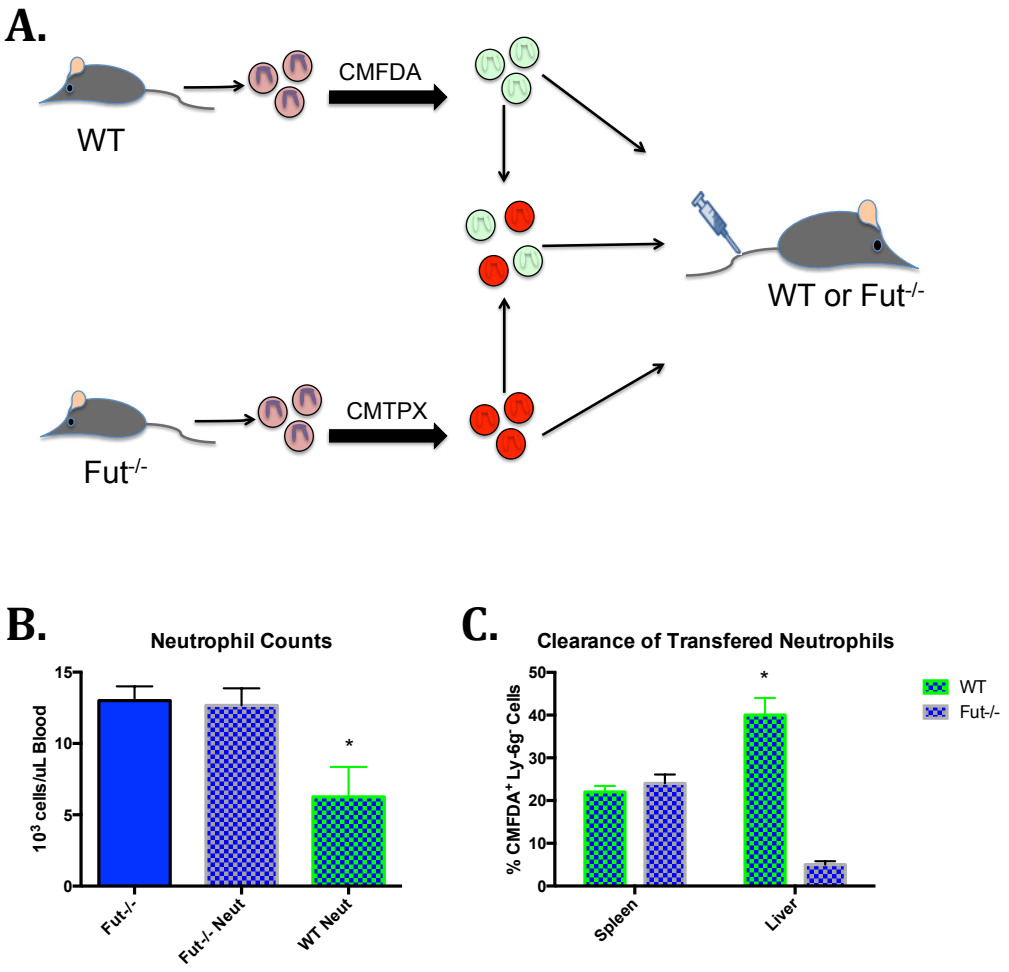

Figure 3.10. Neutrophil Trafficking to the Liver Regulates Granulopoiesis. **A.** Schematic of Adoptive Transfer. Neutrophils were isolated from WT or Fut$^{-/-}$ mice, labeled in vitro and injected mixed or individually in to WT or Fut$^{-/-}$. **B.** Fut$^{-/-}$ mice that were injected with Fut-/- neutrophil had no change in circulating neutrophil counts. WT neutrophils injected into Fut$^{-/-}$ mice reduced circulating neutrophil counts by 50%. **C.** Fut$^{-/-}$ phagocytes were then assessed for CMFDA positivity, which indicated a labeled neutrophil had been engulfed. No difference was observed between Fut$^{-/-}$ splenic macrophages that had engulfed WT or Fut $^{-/-}$labeled neutrophils. However, significantly more Kupffer cells had phagocytized WT neutrophils then Fut$^{-/-}$ neutrophils. n= 7 mice/condition. Data presented as mean ± standard error. *=p≤0.05

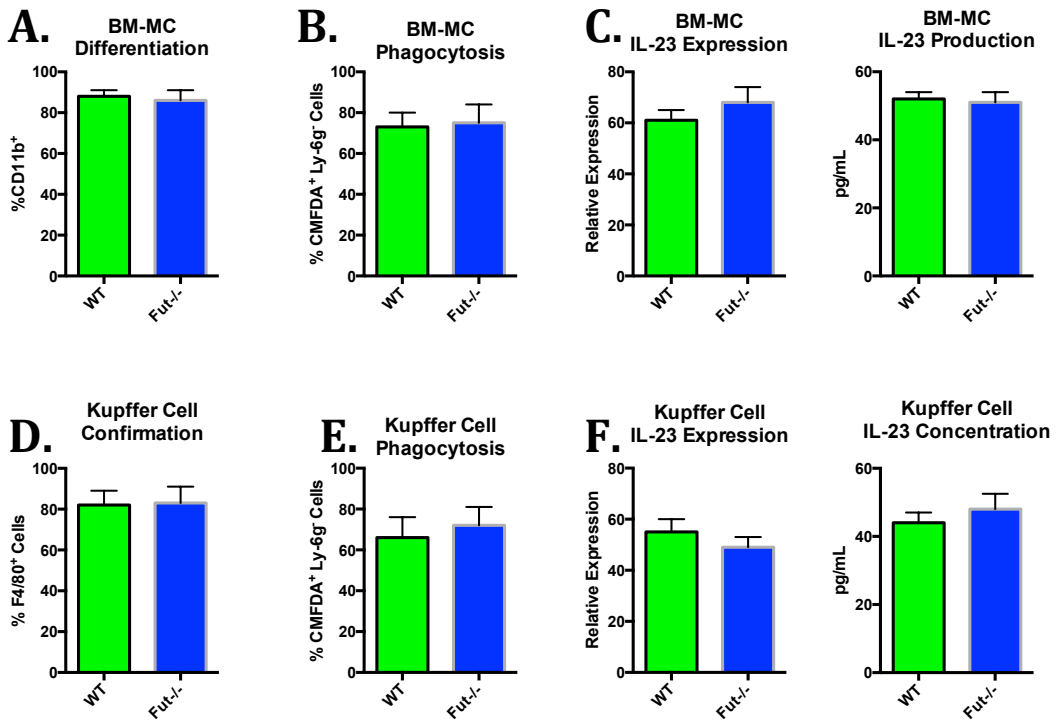

Figure 3.11. Loss of Fut Activity Does Not Inhibit Macrophage Phagocytosis IL-23 Expression or IL-23 Production.

A. BM-MCs were differentiated in RPMI with M-CSF for seven days. Differentiation was confirmed by $CD11B^+$ staining by flow cytometry. There was no difference in percent successful differentiation between WT and $Fut^{-/-}$ BM-MCs. **B.** BM-MCs were then incubated with $1x10^6$ apoptotic neutrophils, for one hour. There was no difference in the number BM-MCs that engulfed at least one neutrophil between WT and $Fut^{-/-}$ BM-MCs. **C.** BM-MCs were stimulated with 10ng/mL LPS for four hours, and mRNA and culture supernatants were isolated. Neither gene expression or protein production of IL-23 was different between WT and $Fut^{-/-}$ BM-MCs. **D.** Primary Kupffer cells (pKCs) were isolated from WT and $Fut^{-/-}$ livers in equal numbers. **E.** WT and $Fut^{-/-}$ pKCs equally phagocytized apoptotic neutrophils, **F.** No difference was observed in IL-23 expression or protein production by kupffer cells following LPS injection. n=6-12 mice / genotype. Data presented as mean ± standard error.

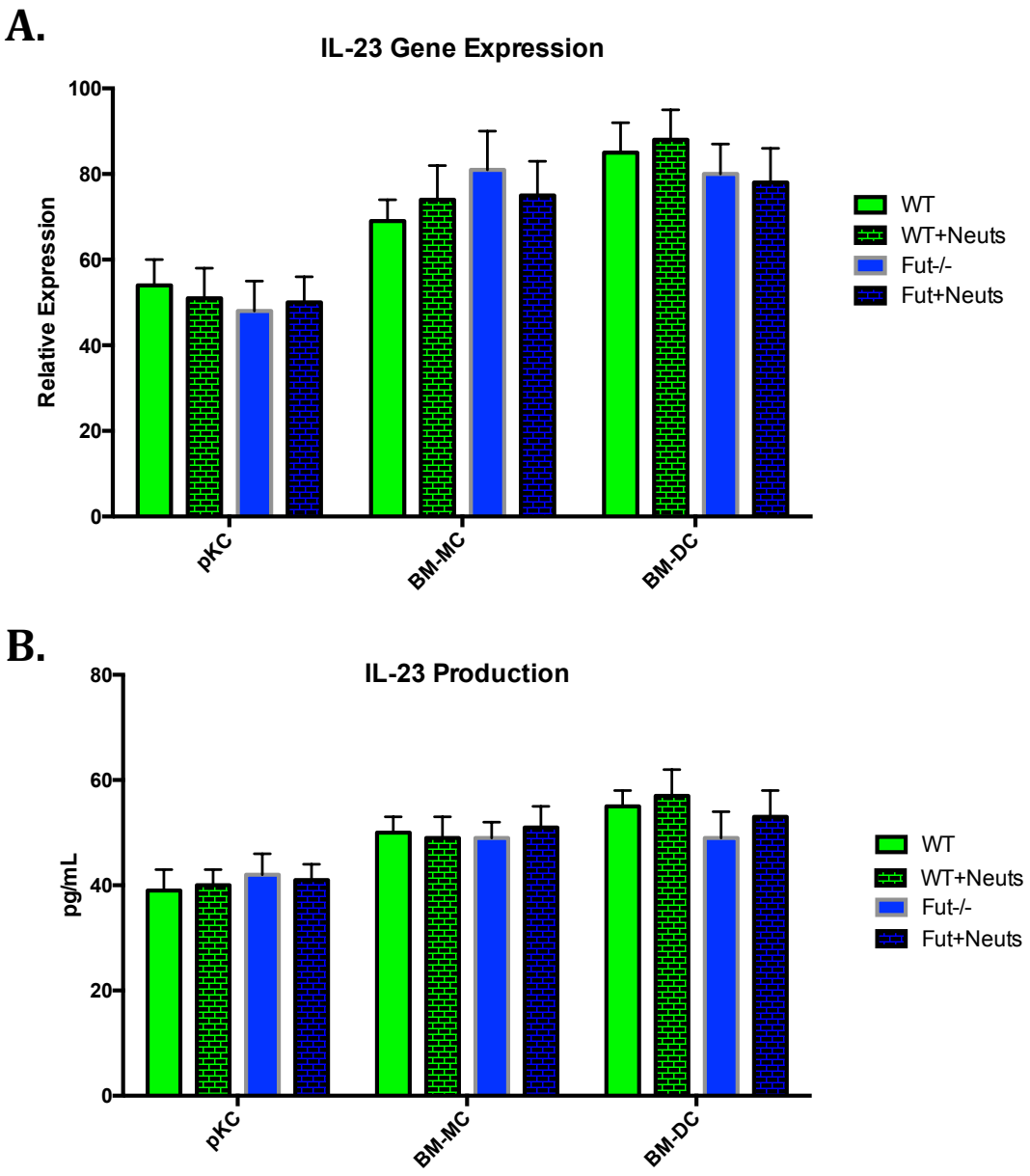

Figure 3.12. Efferocytosis alone is in adequate to suppress IL-23 expression or production.
A. BM-MCs, BM-DCs, and pKCs were isolated from WT and Fut$^{-/-}$ mice, stimulated with LPS to induce IL-23 expression, then incubated with 1x10^{6} apoptotic neutrophils to assess the effects of efferocytosis on IL-23 expression. IL-23 gene expression was induced to similar level in WT and Fut$^{-/-}$ phagocytes. Efferocytosis was unable to suppress IL-23 expression in any WT or Fut$^{-/-}$ pKCs, BM-MCs, or BM-DCs.
B. IL-23 production into cell culture media by WT and Fut$^{-/-}$ pKCs, BM-MCs, and BM-DCs was assed via ELISA. There was no difference between WT and Fut$^{-/-}$ IL-23 production by phagocytes. Efferocytosis was unable to suppress IL-23 production by WT or Fut$^{-/-}$ pKCs, BM-MCs, or BM-DCs. n=6-8 mice/ genotype. Data presented as mean ± standard error.

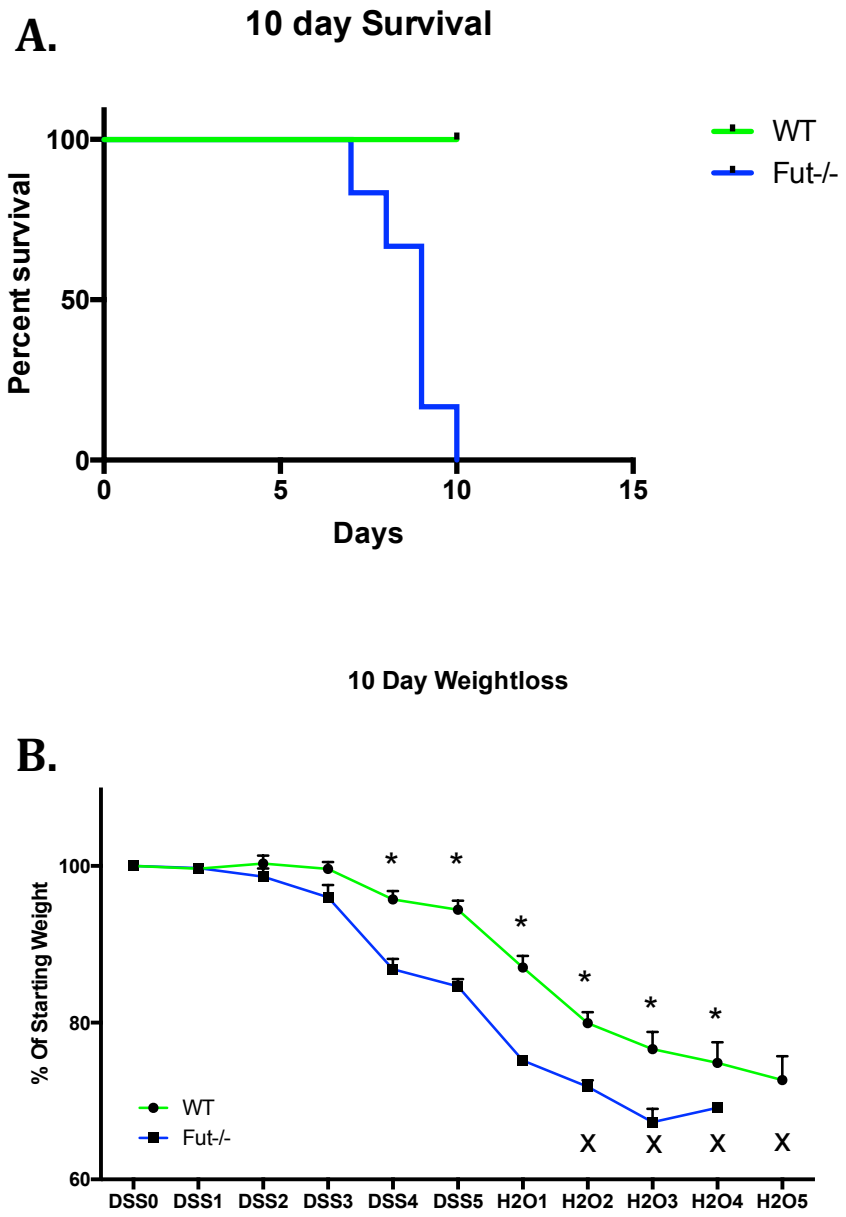

Figure 3.13. 10 Day Time Point: Fut$^{-/-}$ Mice Develop a More Severe Colitis Then WT Mice

A. WT and Fut$^{-/-}$ mice were administered 3% DSS in their drinking water for 5 days followed by 5 days of water for recovery. All Fut$^{-/-}$ mice succumbed before the end of the experiment, while all WT mice lived. **B.** Fut$^{-/-}$ mice lost 15% more weight than WT mice over the course of the experiment. n=8 mice/genotype. Data presented as mean ± standard error. *=p≤0.05, x= loss of at least one mouse

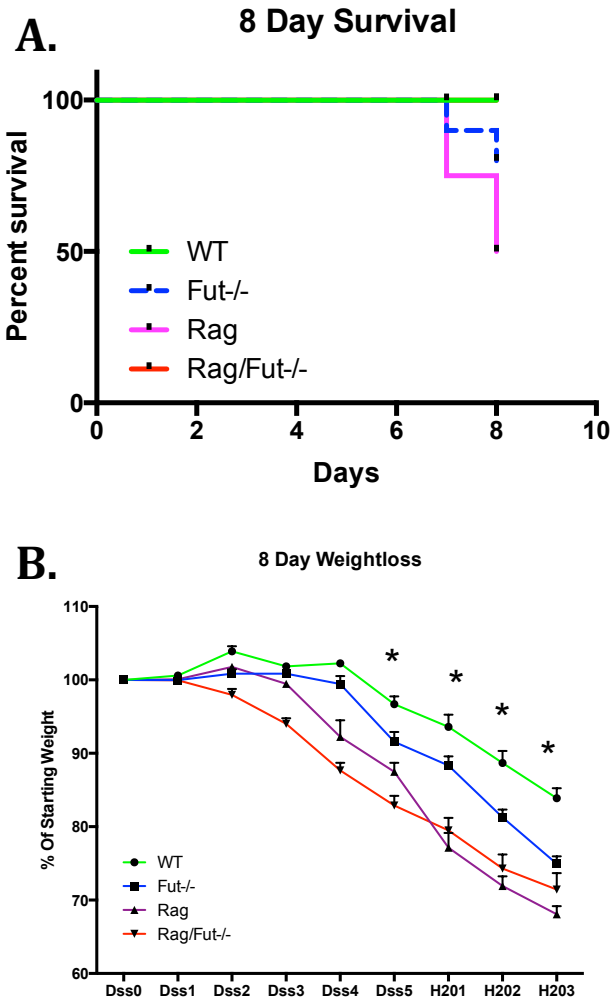

Figure 3.14. 8 Day Time Point: Rag1$^{-/-}$ and Fut$^{-/-}$ mice Develop Severe Colitis

A. WT, Fut$^{-/-}$, Rag1-/- and Rag1$^{-/-}$/Fut$^{-/-}$ mice were given 3% DSS for 5 days followed by 3 days water. 50% Rag1$^{-/-}$ and 20% Fut$^{-/-}$ mice succumbed before the end of the experiment but no WT or Rag1$^{-/-}$/Fut$^{-/-}$ died. **B.** Rag1$^{-/-}$ and Rag1$^{-/-}$/Fut$^{-/-}$ mice lost 20% more weight then WT mice, Fut$^{-/-}$ mice lost 10% more weight then WT mice. **C.** When disease severity was assessed histologically no difference in disease severity was observed among WT, Fut$^{-/-}$ and Rag1$^{-/-}$/Fut$^{-/-}$ mice. Rag1$^{-/-}$ mice however had significantly worse colitis then the other genotypes tested.

n=5-8 mice/genotype. Data presented as mean ± standard error. *=p≤0.05

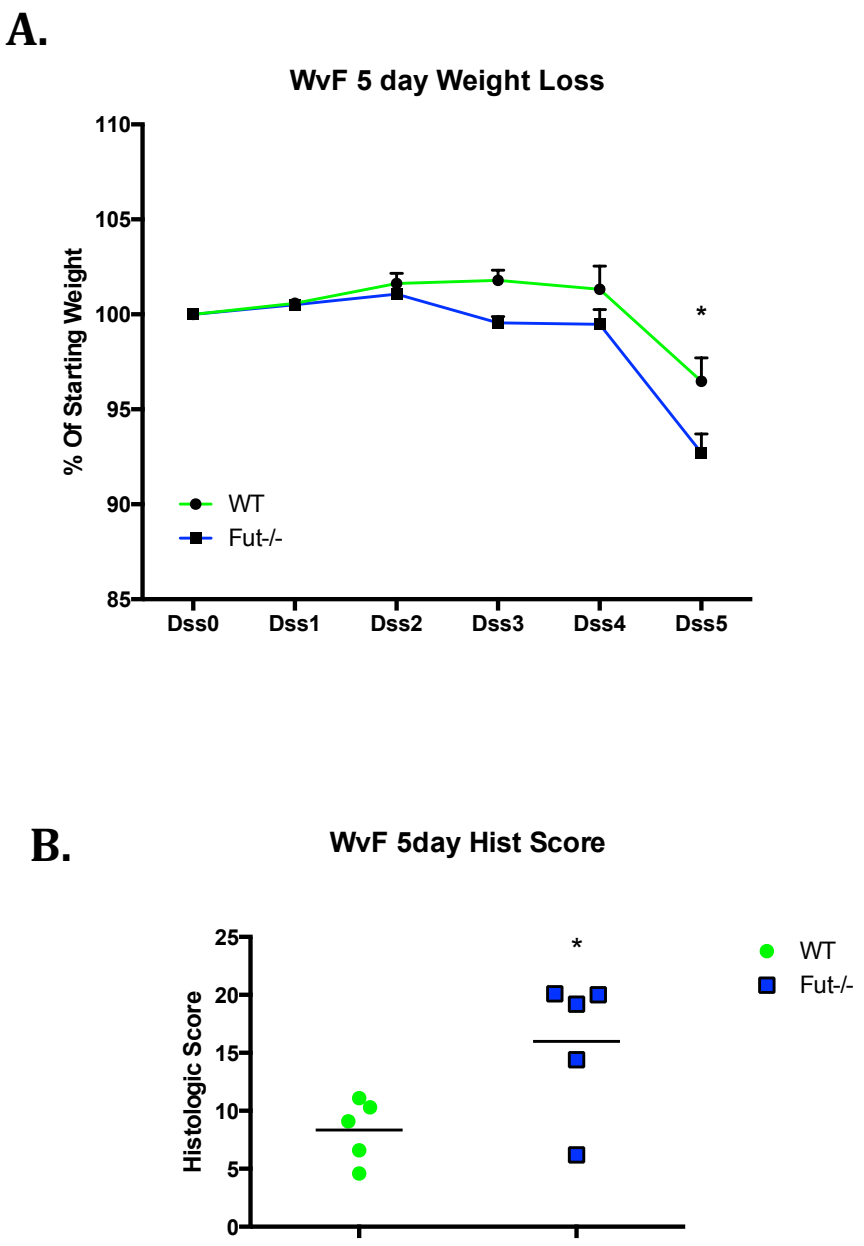

Figure 3.15 – 5 Day Time Point: Fut$^{-/-}$ mice develop more Severe Colitis Then WT Mice

A. WT and Fut$^{-/-}$ mice were given 3% DSS for 5 days. All mice survived to the end of the experiment. Fut$^{-/-}$ mice lost 5% more weight then WT mice. **B.** Fut$^{-/-}$ mice have more severe colitis histologic score then WT

Chapter 4 – Discussion and Significance

4.1 Summary of Main Findings

The findings outlined in Chapter 3 demonstrate the impact α(1,3)-fucosylation-dependent selectin-mediated trafficking of leukocytes can have on homeostatic immunity, granulopoiesis, and mucosal injury. Studies in Chapter 3.1 show that the loss of FUT4 and FUT7 result in a leukocytosis characterized primarily by a pronounced neutrophilia. $Fut^{-/-}$ mice also have expanded populations of IL-17-producing Th17, $\gamma\delta$ Tcell, NKT cells, and ILCs compared to WT mice. I hypothesized that the Fut-dependent expansion of IL-17 producing cells are the result of altered Tcell differentiation, however the results from the *in vitro* Th17 differentiation assay suggest that Tcell differentiation is not altered in $Fut^{-/-}$ mice. In addition to the alterations in circulating neutrophil counts and IL-17-producing Th17, $\gamma\delta$ Tcells, NKT, and ILCs, circulating concentrations of IL-13, IL-17, G-CSF, MCP-1, and MIP-1α are significantly elevated in $Fut^{-/-}$ mice compared to WT mice. All of these findings are primarily dependent on FUT7 activity and were shown to be selectin-dependent.

Chapter 3.2 assessed the role of α(1,3)-fucosylated glycans in regulating granulopoiesis. Injection of α-Ly-6G into $Fut^{-/-}$ mice failed to

deplete circulating neutrophils. Emergency granulopoiesis signaling remains intact, as LPS injection results in significant elevation of circulating neutrophil counts in $Fut^{-/-}$ mice. Studies using the Tg-Fut and Cre-Fut mice showed that the neutrophilia and IL-17 production are dependent on myeloid cell trafficking. The identification of elevated IL-17 production and a marked neutrophilia in $Rag1^{-/-}/Fut^{-/-}$ mice showed that B-cells and Tcells are not required for the maintenance of the neutrophilia and IL-17-producing leukocyte populations identified in $Fut^{-/-}$ mice. Bone marrow transplantation of $Fut^{-/-}$ BM into lethally irradiated WT mice reconstituted the leukocytosis and pronounced neutrophilia and caused expansions in IL-17-producing cell populations. Together, these data show that BM-derived myeloid cell trafficking is required for maintenance of homeostatic granulopoiesis. These results were confirmed by transferring WT BM into lethally irradiated $Fut^{-/-}$ mice, which reconstituted WT number of circulating neutrophils and populations IL-17-producing cells. Finally, the results from the adoptive neutrophil transfer experiments show that Fut-dependent neutrophil trafficking to the liver in part regulates homeostatic granulopoiesis.

In Chapter 3.3, the dependence of intestinal injury on $\alpha(1,3)$-fucosylation-dependent changes in the inflammatory immune response were tested. $Fut^{-/-}$ mice had more severe disease then WT mice at each time point tested in the DSS-induced model colitis. Additionally, at the 8-

day time point, Rag1$^{-/-}$ mice developed more severe disease then WT mice, however the disease severity was reduced in Rag1$^{-/-}$/Fut$^{-/-}$ mice.

4.2 Considerations for the Manipulation of Leukocyte Trafficking

Leukocyte trafficking has long been known to be a vital process for leukocyte maturation, immune surveillance, and response to infection and tissue damage. The findings from our studies reinforce the importance of leukocyte trafficking to the maintenance of circulating leukocyte counts and IL-17 production, and also offer very interesting insights into the effects of manipulating selectin-dependent leukocyte trafficking pharmacologically or otherwise. Our findings demonstrate that inhibition of selectin-dependent trafficking stimulates enhanced granulopoiesis and increased production of IL-17. Several pharmacologic compounds are available or under development to inhibit selectins in humans[97-99]. These drugs seek to reduce inflammation, however, our findings suggest that their use could result in elevated IL-17 production, which has been implicated in autoimmune diseases and IBD. This raises the potential risk of patients developing autoimmune disease or exacerbating other IL-17-dependent inflammatory disease processes. Additionally, loss of selectin-dependent trafficking will cause an increase in granulopoiesis resulting in a neutrophilia. Our findings in a model of colitis indicate that the neutrophilia can potentially increase inflammation and tissue injury even

in the context of the leukocyte trafficking deficiency. $Fut^{-/-}$ neutrophils, macrophages, and Tcells which require Fut-dependent selectin-mediated adhesion events to traffic into tissues, can be isolated from inflamed and damaged tissues under disease conditions such as colitis, atherosclerosis, and contact hypersensitivity reactions. The presence of these cells in the inflamed tissue suggests that under disease conditions the stringency of trafficking requirements into tissues is reduced, potentially due to increased vascular permeability or direct damage to the blood vessels. While the mechanism of $Fut^{-/-}$ leukocyte entry into disease tissues remains unclear, the leukocytes are able to enter the tissues and exacerbate immune pathology.

While the inhibition of all selectin-mediated leukocyte trafficking in Fut-/- or E,P,L-/- mice has severe consequences on circulating leukocyte counts and IL-17 production, functional inhibition of only an individual selectin (i.e. P-selectin) has much less impact on these effects. The results from Chapter 3.1 show that the loss of E-, P-, and L- selectins is required to induce a neutrophilia and elevation in IL-17. Therefore, if a particular disease process is dependent on a single selectin, the data suggest it would be safe to inhibit that selectin to dampen the inflammatory response. It is important to note that all our experiments were conducted in mouse models with a permanent leukocyte trafficking deficiency. Therefore, our results identify systemic changes that occur

after long-term blocking of selectin-dependent leukocyte trafficking. The elevated levels of IL-17 and the neutrophilia resulting from a chronic trafficking deficiency reduces the therapeutic potential of long-term treatments aimed at inhibiting leukocyte trafficking. Short-term treatments may however, provide an anti-inflammatory effect associated with inhibition of leukocyte trafficking without significantly altering IL-17-producing cell numbers, IL-17concentrations, or circulating neutrophil counts.

4.3 Considerations for Our Understanding of the Regulation of Granulopoiesis

Loss of selectin-dependent leukocyte trafficking inhibits neutrophil extravasation, which reduces the clearance of neutrophils by peripheral phagocytes, causing accelerated homeostatic granulopoiesis, resulting in a pronounced neutrophilia. The data partially confirm the granulopoietic regulatory loop proposed by Stark et al[20]. However they also identify additional needed studies. The results in Chapter 3.2 confirm that neutrophil trafficking appears to be required for maintenance of homeostatic granulopoiesis. However, efferocytosis was insufficient to suppress IL-23 expression or production in WT or $Fut^{-/-}$ pKCs, BM-MCs, or BM-DCs in an *in vitro* efferocytosis assay. These findings suggest that there may be additional factors involved in the modulation of IL-23

production. As our adoptive transfer experiments identified that the liver is involved in clearance of neutrophils, we hypothesize that the IL-10 produced by phagocytes following efferocytosis simulates hepatocytes to produce IL-25. IL-25 has been shown to be a potent inhibitor of IL-23 production[100-103]. This as yet untested alternate mechanism may explain why we were unable to suppress IL-23 in our in vitro efferocytosis assay.

In addition, our bio-plex data shows that circulating IL-23 levels are not elevated in Fut-/- mice under steady-state or LPS-injected conditions. The lack of altered circulating IL-23 concentrations suggests that either additional cytokines or growth factors may be involved in the proliferation of IL-17 producing cell populations or that local IL-23 concentration changes can regulate granulopoiesis without affecting systemic circulating IL-23 concentrations. Taken together, these findings demonstrate that the model of granulopoiesis regulation proposed by Stark et al., is incomplete. We propose an updated model (Figure 4.1) for the regulation of granulopoiesis. This model reflects the observations we have made and highlights areas within the regulatory loop in need of further research. Specifically, 1) the precise stimulus responsible for inducing macrophage IL-23 production needs to be elucidated, 2) the additional cytokine or growth factors involved in the proliferation of IL-17-producing cells need to be determined, and 3) the intracellular signaling events

activated by efferocytosis and responsible for IL-10 production need to be studied.

Recent studies determined that TRM are distinct populations of phagocytes that infiltrate into tissues during embryonic development, and that are maintained independent from the BM through adulthood[5, 70, 72, 78]. The trafficking requirements for TRM progenitors have not been studied. Our findings demonstrate that similar numbers of pKCs can be isolated from the liver of WT and $Fut^{-/-}$ mice. These results suggest that the trafficking of fetal hematopoietic progenitors responsible for establishing Kupffer cell populations is not dependent on selectin-ligand function.

While the role for selectins in macrophage phagocytosis, efferocytosis, and IL-23 production have not been described, our findings demonstrate that macrophages from $Fut^{-/-}$ mice do not have a defect in phagocytic rate, IL-23 gene expression, or IL-23 production. These results show that recognition and phagocytosis of apoptotic neutrophils is independent of fucosylation-dependent selectin ligand activity, and likely depends on macrophage recognition of phosphatidylserine displayed on the outer plasma membrane of apoptotic neutrophils, or another Fut-independent process.

4.4 Considerations for Leukocyte Adhesion Deficiency Type II

These results have important implications for patients with Leukocyte Adhesion Deficiency II. LADII patients have a deficiency in the enzymes responsible for the production of UDP-fucose, the substrate for the fucosyltransferases including Fut4 and Fut7. This deficiency in LADII results in a loss of fucosylated glycoproteins including the selectin ligands. LADII patients have a leukocytosis with a pronounced neutrophilia[4, 104, 105]. Our results suggest that LADII patients will have increased number of IL-17-producing Th17, γδ Tcell, NKT, and ILCs, increased circulating IL-17 and G-CSF concentrations, and accelerated granulopoiesis. These alterations create an altered immune environment that may predispose LADII patients to disease. Specifically, elevated IL-17 concentrations have been associated with an increased prevalence and severity of autoimmune diseases such as multiple sclerosis, psoriasis, asthma, and lupus. Despite the fucosylation-dependent leukocyte trafficking deficiency, our data suggest that LADII patients will have normal populations of TRMs that are fully capable of phagocytosing cellular debris and producing cytokines.

4.5 Understanding the Pathogenesis of Mucosal Injury in Colitis

Acute DSS-induced colitis is thought to be a granulocyte-dependent disease process[85-88, 95]. Therefore, we were surprised to find that

Fut$^{-/-}$ mice, which have a marked granulocyte trafficking deficiency had more severe colitis then WT mice. These results suggest that the elevations in IL-17 and the higher numbers of circulating neutrophils enhanced disease pathogenesis more then the protection afforded by the loss of fucosylation-dependent selectin-mediated leukocyte trafficking. These experiments are unable to determine whether the IL-17 or the neutrophilia is responsible for increased disease severity, or their relative contributions to the disease process.

Rag1$^{-/-}$ mice develop severe DSS-induced colitis[84-88]. Therefore, Bcells and Tcells are not required for the induction of colitis. In our experiments Rag1$^{-/-}$ had more severe colitis then WT or Fut$^{-/-}$ mice suggesting that lymphocytes (Bregs and Tregs) may inhibit inflammation and reduce disease severity. However when colitis in Rag1$^{-/-}$/Fut$^{-/-}$ mice was assessed, the disease severity was reduced compared to Rag1$^{-/-}$, and was similar to disease severity in WT and Fut$^{-/-}$ mice at the eight day time point. Rag1$^{-/-}$ mice do not have a pronounced neutrophilia or elevated IL-17 like Fut$^{-/-}$ mice, so these findings are difficult to interpret. Our findings suggest that a non-lymphoid inflammatory cell exacerbates the severity of colitis in Rag1$^{-/-}$ mice, and that these inflammatory cells rely on Fut–dependent selectin-mediated trafficking to enter colon and drive inflammation. This would account for the loss of enhanced disease severity in Rag1$^{-/-}$/Fut$^{-/-}$ mice.

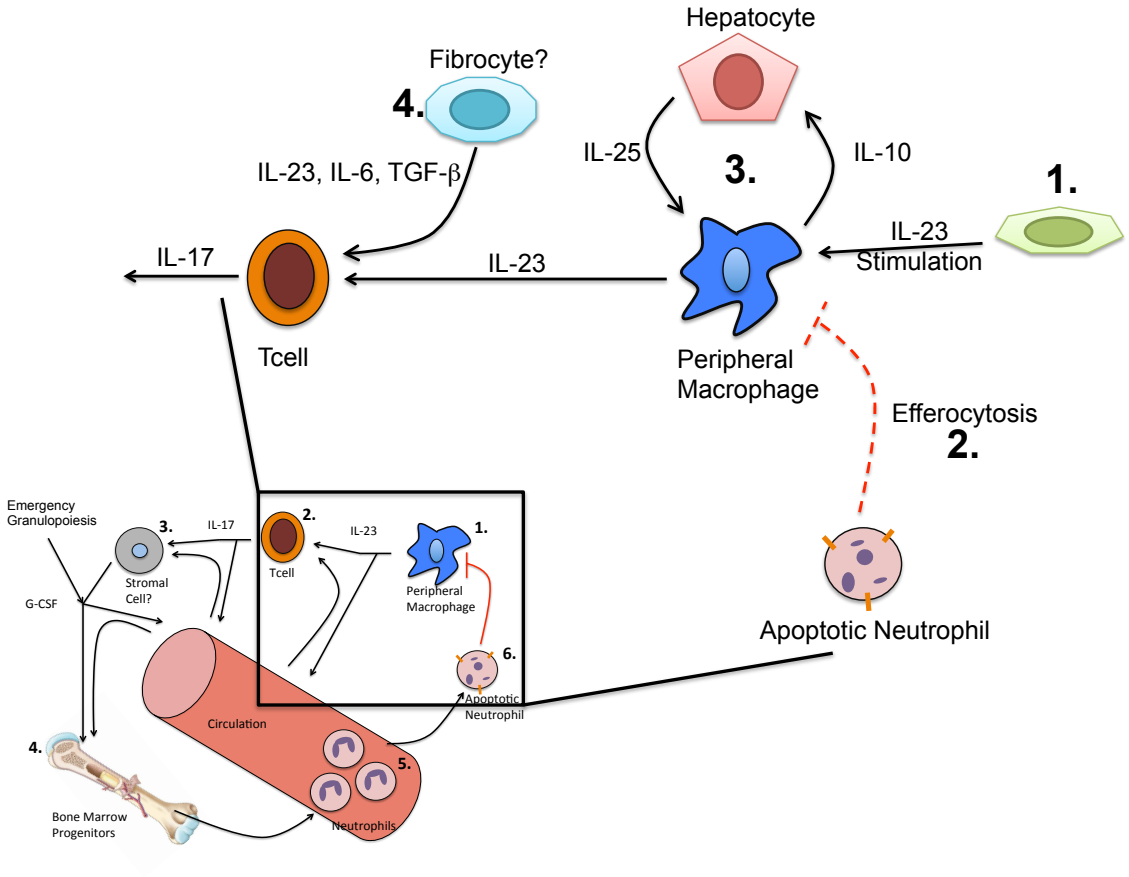

Figure 4.1 – Updated Model of the Regulation of Granulopoiesis
The results from our studies have shown that the existing model for the regulation of granulopoiesis is incomplete. **1.** Our in vitro experiments demonstrated that phagocytes do not produce IL-23 without LPS stimulation. These data suggest that in vivo there is an unidentified stimulating factor responsible for IL-23 production by macrophages and dendritic cells. **2.** The in vitro efferocytosis (IVE) assays showed that efferocytosis alone was not sufficient to suppress IL-23 gene expression or protein production. **3.** Additionally, the IVE studies revealed that following efferocytosis macrophages produced copious amounts of IL-10. These observations coupled with the results from our adoptive transfer experiments led us to hypothesize that additional factors may be involved in the suppression of IL-23. One potential factor is IL-25 ,which is a potent inhibitor of IL-23, and is produced by hepatocytes in response to IL-10. **4.** We were unable to detect alterations in circulating IL-23 levels in vivo in Fut$^{-/-}$ mice. This suggests that either local changes in IL-23 may be sufficient to modulate IL-17 production without affecting circulating IL-23 concentrations, or that a different factor may be involved in driving IL-17 production in Fut$^{-/-}$ mice. One potential source of IL-17 induction could be from fibrocytes. These cells have been shown to stimulate IL-17 production, and even produce IL-17 themselves in response to IL-13, which is elevated in Fut$^{-/-}$ mice.

REFERNCES

1. Homeister, J.W., et al., *The alpha(1,3)fucosyltransferases FucT-IV and FucT-VII exert collaborative control over selectin-dependent leukocyte recruitment and lymphocyte homing.* Immunity, 2001. **15**(1): p. 115-26.

2. de Vries, T., et al., *Fucosyltransferases: structure/function studies.* Glycobiology, 2001. **11**(10): p. 119R-128R.

3. Li, W., et al., *Core fucosylation of mu heavy chains regulates assembly and intracellular signaling of precursor B cell receptors.* J Biol Chem, 2012. **287**(4): p. 2500-8.

4. Luhn, K. and M.K. Wild, *Human deficiencies of fucosylation and sialylation affecting selectin ligands.* Semin Immunopathol, 2012. **34**(3): p. 383-99.

5. Davies, L.C., et al., *Tissue-resident macrophages.* Nat Immunol, 2013. **14**(10): p. 986-95.

6. Manz, M.G. and S. Boettcher, *Emergency granulopoiesis.* Nat Rev Immunol, 2014. **14**(5): p. 302-14.

7. Ley, K. and G.S. Kansas, *Selectins in T-cell recruitment to non-lymphoid tissues and sites of inflammation.* Nat Rev Immunol, 2004. **4**(5): p. 325-35.

8. Smithson, G., et al., *Fuc-TVII is required for T helper 1 and T cytotoxic 1 lymphocyte selectin ligand expression and recruitment in inflammation, and together with Fuc-TIV regulates naive T cell trafficking to lymph nodes.* J Exp Med, 2001. **194**(5): p. 601-14.

9. Wang, H., et al., *alpha(1,3)-Fucosyltransferases FUT4 and FUT7 control murine susceptibility to thrombosis.* Am J Pathol, 2013. **182**(6): p. 2082-93.

10. Gaffen, S.L., *Recent advances in the IL-17 cytokine family.* Curr Opin Immunol, 2011. **23**(5): p. 613-9.

11. Wirths, S., S. Bugl, and H.G. Kopp, *Steady-state neutrophil homeostasis is a demand-driven process.* Cell Cycle, 2013. **12**(5): p. 709-10.

12. Wirths, S., S. Bugl, and H.G. Kopp, *Neutrophil homeostasis and its regulation by danger signaling.* Blood, 2014.

13. Wright, H.L., et al., *Neutrophil function in inflammation and inflammatory diseases.* Rheumatology (Oxford), 2010. **49**(9): p. 1618-31.

14. Bugl, S., et al., *Current insights into neutrophil homeostasis.* Ann N Y Acad Sci, 2012. **1266**: p. 171-8.

15. Bugl, S., et al., *Steady-state neutrophil homeostasis is dependent on TLR4/TRIF signaling.* Blood, 2013. **121**(5): p. 723-33.

16. Elghetany, M.T., et al., *Flow cytometric study of neutrophilic granulopoiesis in normal bone marrow using an expanded panel of antibodies: correlation with morphologic assessments.* J Clin Lab Anal, 2004. **18**(1): p. 36-41.

17. Gordy, C., et al., *Regulation of steady-state neutrophil homeostasis by macrophages.* Blood, 2011. **117**(2): p. 618-29.

18. Fox, S., et al., *Neutrophil apoptosis: relevance to the innate immune response and inflammatory disease.* J Innate Immun, 2010. **2**(3): p. 216-27.

19. Daley, J.M., et al., *Use of Ly6G-specific monoclonal antibody to deplete neutrophils in mice.* J Leukoc Biol, 2008. **83**(1): p. 64-70.

20. Stark, M.A., et al., *Phagocytosis of apoptotic neutrophils regulates granulopoiesis via IL-23 and IL-17.* Immunity, 2005. **22**(3): p. 285-94.

21. Smith, E., et al., *IL-17A inhibits the expansion of IL-17A-producing T cells in mice through "short-loop" inhibition via IL-17 receptor.* J Immunol, 2008. **181**(2): p. 1357-64.

22. Ley, K., E. Smith, and M.A. Stark, *IL-17A-producing neutrophil-regulatory Tn lymphocytes.* Immunol Res, 2006. **34**(3): p. 229-42.

23. von Vietinghoff, S., H. Ouyang, and K. Ley, *Mycophenolic acid suppresses granulopoiesis by inhibition of interleukin-17 production.* Kidney Int, 2010. **78**(1): p. 79-88.

24. Smith, E., et al., *T-lineage cells require the thymus but not VDJ recombination to produce IL-17A and regulate granulopoiesis in vivo.* J Immunol, 2009. **183**(9): p. 5685-93.

25. Panopoulos, A.D. and S.S. Watowich, *Granulocyte colony-stimulating factor: molecular mechanisms of action during steady state and 'emergency' hematopoiesis.* Cytokine, 2008. **42**(3): p. 277-88.

26. Wright, H.L., et al., *Changes in expression of membrane TNF, NF-{kappa}B activation and neutrophil apoptosis during active and resolved inflammation.* Ann Rheum Dis, 2011. **70**(3): p. 537-43.

27. Michlewska, S., et al., *Macrophage phagocytosis of apoptotic neutrophils is critically regulated by the opposing actions of pro-inflammatory and anti-inflammatory agents: key role for TNF-alpha.* FASEB J, 2009. **23**(3): p. 844-54.

28. Korns, D., et al., *Modulation of macrophage efferocytosis in inflammation.* Front Immunol, 2011. **2**: p. 57.

29. Yang, Y., et al., *Urokinase-type plasminogen activator inhibits efferocytosis of neutrophils.* Am J Respir Crit Care Med, 2010. **182**(12): p. 1516-23.

30. Weisser, S.B., N. van Rooijen, and L.M. Sly, *Depletion and reconstitution of macrophages in mice.* J Vis Exp, 2012(66): p. 4105.

31. Shearn, A.I., et al., *Bcl-x inactivation in macrophages accelerates progression of advanced atherosclerotic lesions in Apoe(-/-) mice.* Arterioscler Thromb Vasc Biol, 2012. **32**(5): p. 1142-9.

32. Friggeri, A., et al., *Participation of the receptor for advanced glycation end products in efferocytosis.* J Immunol, 2011. **186**(11): p. 6191-8.

33. Banerjee, S., et al., *The C-terminal acidic tail is responsible for the inhibitory effects of HMGB1 on efferocytosis.* J Leukoc Biol, 2010. **88**(5): p. 973-9.

34. Banerjee, S., et al., *Intracellular HMGB1 negatively regulates efferocytosis.* J Immunol, 2011. **187**(9): p. 4686-94.

35. Friggeri, A., et al., *HMGB1 inhibits macrophage activity in efferocytosis through binding to the alphavbeta3-integrin.* Am J Physiol Cell Physiol, 2010. **299**(6): p. C1267-76.

36. Vignali, D.A. and V.K. Kuchroo, *IL-12 family cytokines: immunological playmakers.* Nat Immunol, 2012. **13**(8): p. 722-8.

37. Liu, B., et al., *IL-17 is a potent synergistic factor with GM-CSF in mice in stimulating myelopoiesis, dendritic cell expansion, proliferation, and functional enhancement.* Exp Hematol, 2010. **38**(10): p. 877-884 e1.

38. Yannam, G.R., T. Gutti, and L.Y. Poluektova, *IL-23 in infections, inflammation, autoimmunity and cancer: possible role in HIV-1 and AIDS.* J Neuroimmune Pharmacol, 2012. **7**(1): p. 95-112.

39. Wu, Q., et al., *IL-23-dependent IL-17 production is essential in neutrophil recruitment and activity in mouse lung defense against respiratory Mycoplasma pneumoniae infection.* Microbes Infect, 2007. **9**(1): p. 78-86.

40. Jones, L.L., et al., *Distinct subunit pairing criteria within the heterodimeric IL-12 cytokine family.* Mol Immunol, 2012. **51**(2): p. 234-44.

41. Ivanov, S., et al., *Functional relevance of the IL-23-IL-17 axis in lungs in vivo.* Am J Respir Cell Mol Biol, 2007. **36**(4): p. 442-51.

42. Huang, G., et al., *Signaling via the kinase p38alpha programs dendritic cells to drive TH17 differentiation and autoimmune inflammation.* Nat Immunol, 2012. **13**(2): p. 152-61.

43. Cao, H., et al., *Anti-IL-23 antibody blockade of IL-23/IL-17 pathway attenuates airway obliteration in rat orthotopic tracheal transplantation.* Int Immunopharmacol, 2011. **11**(5): p. 569-75.

44. Uhlig, H.H., et al., *Differential activity of IL-12 and IL-23 in mucosal and systemic innate immune pathology.* Immunity, 2006. **25**(2): p. 309-18.

45. Griffin, G.K., et al., *IL-17 and TNF-alpha sustain neutrophil recruitment during inflammation through synergistic effects on endothelial activation.* J Immunol, 2012. **188**(12): p. 6287-99.

46. Sheibanie, A.F., et al., *Prostaglandin E2 induces IL-23 production in bone marrow-derived dendritic cells.* FASEB J, 2004. **18**(11): p. 1318-20.

47. Ivanov, II, et al., *The orphan nuclear receptor RORgammat directs the differentiation program of proinflammatory IL-17+ T helper cells.* Cell, 2006. **126**(6): p. 1121-33.

48. Vantourout, P. and A. Hayday, *Six-of-the-best: unique contributions of gammadelta T cells to immunology.* Nat Rev Immunol, 2013. **13**(2): p. 88-100.

49. Meyer, C., X. Zeng, and Y.H. Chien, *Ligand recognition during thymic development and gammadelta T cell function specification.* Semin Immunol, 2010. **22**(4): p. 207-13.

50. Guan, H., P.S. Nagarkatti, and M. Nagarkatti, *CD44 Reciprocally regulates the differentiation of encephalitogenic Th1/Th17 and Th2/regulatory T cells through epigenetic modulation involving DNA methylation of cytokine gene promoters, thereby controlling the development of experimental autoimmune encephalomyelitis.* J Immunol, 2011. **186**(12): p. 6955-64.

51. Tan, W., et al., *IL-17F/IL-17R interaction stimulates granulopoiesis in mice.* Exp Hematol, 2008. **36**(11): p. 1417-27.

52. Tam, S., et al., *IL-17 and gammadelta T-lymphocytes play a critical role in innate immunity against Nocardia asteroides GUH-2.* Microbes Infect, 2012. **14**(13): p. 1133-43.

53. Kappel, L.W., et al., *IL-17 contributes to CD4-mediated graft-versus-host disease.* Blood, 2009. **113**(4): p. 945-52.

54. Grace, M.B., et al., *5-AED enhances survival of irradiated mice in a G-CSF-dependent manner, stimulates innate immune cell function, reduces radiation-induced DNA damage and induces genes that modulate cell cycle progression and apoptosis.* J Radiat Res, 2012. **53**(6): p. 840-53.

55. Zhang, H., et al., *STAT3 controls myeloid progenitor growth during emergency granulopoiesis.* Blood, 2010. **116**(14): p. 2462-71.

56. Nguyen-Jackson, H., et al., *STAT3 controls the neutrophil migratory response to CXCR2 ligands by direct activation of G-CSF-induced CXCR2 expression and via modulation of CXCR2 signal transduction.* Blood, 2010. **115**(16): p. 3354-63.

57. McLemore, M.L., et al., *STAT-3 activation is required for normal G-CSF-dependent proliferation and granulocytic differentiation.* Immunity, 2001. **14**(2): p. 193-204.

58. Hirai, H., et al., *C/EBPbeta is required for 'emergency' granulopoiesis.* Nat Immunol, 2006. **7**(7): p. 732-9.

59. Zhang, P., et al., *Induction of granulocytic differentiation by 2 pathways.* Blood, 2002. **99**(12): p. 4406-12.

60. Boettcher, S., et al., *Cutting edge: LPS-induced emergency myelopoiesis depends on TLR4-expressing nonhematopoietic cells.* J Immunol, 2012. **188**(12): p. 5824-8.

61. Akagi, T., et al., *Impaired response to GM-CSF and G-CSF, and enhanced apoptosis in C/EBPbeta-deficient hematopoietic cells.* Blood, 2008. **111**(6): p. 2999-3004.

62. Zhang, P., et al., *Enhancement of hematopoietic stem cell repopulating capacity and self-renewal in the absence of the transcription factor C/EBP alpha.* Immunity, 2004. **21**(6): p. 853-63.

63. Zhang, P., et al., *Upregulation of interleukin 6 and granulocyte colony-stimulating factor receptors by transcription factor CCAAT enhancer binding protein alpha (C/EBP alpha) is critical for granulopoiesis.* J Exp Med, 1998. **188**(6): p. 1173-84.

64. Zhang, D.E., et al., *Absence of granulocyte colony-stimulating factor signaling and neutrophil development in CCAAT enhancer binding protein alpha-deficient mice.* Proc Natl Acad Sci U S A, 1997. **94**(2): p. 569-74.

65. Satake, S., et al., *C/EBPbeta is involved in the amplification of early granulocyte precursors during candidemia-induced "emergency" granulopoiesis.* J Immunol, 2012. **189**(9): p. 4546-55.

66. Cain, D.W., et al., *Inflammation triggers emergency granulopoiesis through a density-dependent feedback mechanism.* PLoS One, 2011. **6**(5): p. e19957.

67. Collins, S.J., et al., *Multipotent hematopoietic cell lines derived from C/EBPalpha(-/-) knockout mice display granulocyte macrophage-colony-stimulating factor, granulocyte- colony-stimulating factor, and retinoic acid-induced granulocytic differentiation.* Blood, 2001. **98**(8): p. 2382-8.

68. Cebon, J., et al., *Endogenous haemopoietic growth factors in neutropenia and infection.* Br J Haematol, 1994. **86**(2): p. 265-74.

69. Bartocci, A., et al., *Macrophages specifically regulate the concentration of their own growth factor in the circulation.* Proc Natl Acad Sci U S A, 1987. **84**(17): p. 6179-83.

70. Wynn, T.A., A. Chawla, and J.W. Pollard, *Macrophage biology in development, homeostasis and disease.* Nature, 2013. **496**(7446): p. 445-55.

71. Zigmond, E. and S. Jung, *Intestinal macrophages: well educated exceptions from the rule.* Trends Immunol, 2013. **34**(4): p. 162-8.

72. Tay, S.S., et al., *The Skin-Resident Immune Network.* Curr Dermatol Rep, 2014. **3**: p. 13-22.

73. Sojka, D.K., et al., *Tissue-resident natural killer (NK) cells are cell lineages distinct from thymic and conventional splenic NK cells.* Elife, 2014. **3**: p. e01659.

74. Labonte, A.C., A.C. Tosello-Trampont, and Y.S. Hahn, *The role of macrophage polarization in infectious and inflammatory diseases.* Mol Cells, 2014. **37**(4): p. 275-85.

75. Gautier, E.L., et al., *Gene-expression profiles and transcriptional regulatory pathways that underlie the identity and diversity of mouse tissue macrophages.* Nat Immunol, 2012. **13**(11): p. 1118-28.

76. Boltjes, A. and F. van Wijk, *Human Dendritic Cell Functional Specialization in Steady-State and Inflammation.* Front Immunol, 2014. **5**: p. 131.

77. Bain, C.C., et al., *Resident and pro-inflammatory macrophages in the colon represent alternative context-dependent fates of the same Ly6Chi monocyte precursors.* Mucosal Immunol, 2013. **6**(3): p. 498-510.

78. Schulz, C., et al., *A lineage of myeloid cells independent of Myb and hematopoietic stem cells.* Science, 2012. **336**(6077): p. 86-90.

79. Hoeffel, G., et al., *Adult Langerhans cells derive predominantly from embryonic fetal liver monocytes with a minor contribution of yolk sac-derived macrophages.* J Exp Med, 2012. **209**(6): p. 1167-81.

80. Hashimoto, D., et al., *Tissue-resident macrophages self-maintain locally throughout adult life with minimal contribution from circulating monocytes.* Immunity, 2013. **38**(4): p. 792-804.

81. Farache, J., et al., *Contributions of dendritic cells and macrophages to intestinal homeostasis and immune defense.* Immunol Cell Biol, 2013. **91**(3): p. 232-9.

82. Michael, D.R., et al., *Differential regulation of macropinocytosis in macrophages by cytokines: implications for foam cell formation and atherosclerosis.* Cytokine, 2013. **64**(1): p. 357-61.

83. Gundra, U.M., et al., *Alternatively activated macrophages derived from monocytes and tissue macrophages are phenotypically and functionally distinct.* Blood, 2014. **123**(20): p. e110-22.

84. Perse, M. and A. Cerar, *Dextran sodium sulphate colitis mouse model: traps and tricks.* J Biomed Biotechnol, 2012. **2012**: p. 718617.

85. Wirtz, S., et al., *Chemically induced mouse models of intestinal inflammation.* Nat Protoc, 2007. **2**(3): p. 541-6.

86. Tlaskalova-Hogenova, H., et al., *Involvement of innate immunity in the development of inflammatory and autoimmune diseases.* Ann N Y Acad Sci, 2005. **1051**: p. 787-98.

87. Dieleman, L.A., et al., *Dextran sulfate sodium-induced colitis occurs in severe combined immunodeficient mice.* Gastroenterology, 1994. **107**(6): p. 1643-52.

88. Chassaing, B., et al., *Dextran sulfate sodium (DSS)-induced colitis in mice.* Curr Protoc Immunol, 2014. **104**: p. Unit 15 25.

89. Mombaerts, P., et al., *RAG-1-deficient mice have no mature B and T lymphocytes.* Cell, 1992. **68**(5): p. 869-77.

90. Liu, Z., et al., *Interleukin (IL)-23 suppresses IL-10 in inflammatory bowel disease.* J Biol Chem, 2012. **287**(5): p. 3591-7.

91. Zheng, Y., et al., *Interleukin-22, a T(H)17 cytokine, mediates IL-23-induced dermal inflammation and acanthosis.* Nature, 2007. **445**(7128): p. 648-51.

92. Liu, Z., et al., *The increased expression of IL-23 in inflammatory bowel disease promotes intraepithelial and lamina propria lymphocyte inflammatory responses and cytotoxicity.* J Leukoc Biol, 2011. **89**(4): p. 597-606.

93. Kitani, H., et al., *A novel isolation method for macrophage-like cells from mixed primary cultures of adult rat liver cells.* J Immunol Methods, 2010. **360**(1-2): p. 47-55.

94. Movita, D., et al., *Kupffer cells express a unique combination of phenotypic and functional characteristics compared with splenic and peritoneal macrophages.* J Leukoc Biol, 2012. **92**(4): p. 723-33.

95. Williams, K.L., et al., *Enhanced survival and mucosal repair after dextran sodium sulfate-induced colitis in transgenic mice that overexpress growth hormone.* Gastroenterology, 2001. **120**(4): p. 925-37.

96. Lubberts, E., et al., *Requirement of IL-17 receptor signaling in radiation-resistant cells in the joint for full progression of destructive synovitis.* J Immunol, 2005. **175**(5): p. 3360-8.

97. Lefer, D.J., *Pharmacology of selectin inhibitors in ischemia/reperfusion states.* Annu Rev Pharmacol Toxicol, 2000. **40**: p. 283-94.

98. Matsui, N.M., A. Varki, and S.H. Embury, *Heparin inhibits the flow adhesion of sickle red blood cells to P-selectin.* Blood, 2002. **100**(10): p. 3790-6.

99. Varki, N.M. and A. Varki, *Heparin inhibition of selectin-mediated interactions during the hematogenous phase of carcinoma metastasis: rationale for clinical studies in humans.* Semin Thromb Hemost, 2002. **28**(1): p. 53-66.

100. Croxford, A.L., F. Mair, and B. Becher, *IL-23: one cytokine in control of autoimmunity.* Eur J Immunol, 2012. **42**(9): p. 2263-73.

101. Rizzo, A., et al., *Inhibition of colitis by IL-25 associates with induction of alternatively activated macrophages.* Inflamm Bowel Dis, 2012. **18**(3): p. 449-59.

102. Sarra, M., et al., *IL-25 prevents and cures fulminant hepatitis in mice through a myeloid-derived suppressor cell-dependent mechanism.* Hepatology, 2013. **58**(4): p. 1436-50.

103. Su, J., et al., *IL-25 downregulates Th1/Th17 immune response in an IL-10-dependent manner in inflammatory bowel disease.* Inflamm Bowel Dis, 2013. **19**(4): p. 720-8.

104. Hidalgo, A., et al., *Insights into leukocyte adhesion deficiency type 2 from a novel mutation in the GDP-fucose transporter gene.* Blood, 2003. **101**(5): p. 1705-12.

105. Luhn, K., et al., *Discontinuation of fucose therapy in LADII causes rapid loss of selectin ligands and rise of leukocyte counts.* Blood, 2001. **97**(1): p. 330-2.